



**HAL**  
open science

## Microplastic fluxes in a large and a small Mediterranean river catchments: The Têt and the Rhône, Northwestern Mediterranean Sea

Mel Constant, Wolfgang Ludwig, Philippe Kerhervé, Jennifer Sola, Bruno Charrière, Anna Sanchez-Vidal, Miquel Canals, Serge Heussner

### ► To cite this version:

Mel Constant, Wolfgang Ludwig, Philippe Kerhervé, Jennifer Sola, Bruno Charrière, et al.. Microplastic fluxes in a large and a small Mediterranean river catchments: The Têt and the Rhône, Northwestern Mediterranean Sea. *Science of the Total Environment*, 2020, 10.1016/j.scitotenv.2020.136984 . hal-03024569

**HAL Id: hal-03024569**

**<https://hal.science/hal-03024569>**

Submitted on 30 Nov 2020

**HAL** is a multi-disciplinary open access archive for the deposit and dissemination of scientific research documents, whether they are published or not. The documents may come from teaching and research institutions in France or abroad, or from public or private research centers.

L'archive ouverte pluridisciplinaire **HAL**, est destinée au dépôt et à la diffusion de documents scientifiques de niveau recherche, publiés ou non, émanant des établissements d'enseignement et de recherche français ou étrangers, des laboratoires publics ou privés.

1 **Microplastic fluxes in a large and a small Mediterranean river catchments: the Têt**  
2 **and the Rhône, Northwestern Mediterranean Sea**

3 Mel Constant, Wolfgang Ludwig, Philippe Kerhervé, Jennifer Sola, Bruno Charrière, Anna Sanchez-  
4 Vidal, Miquel Canals, Serge Heussner.

5 **Abstract**

6 This paper aims at quantifying current riverine fluxes of microplastics (MPs) in two Mediterranean  
7 river catchments, a large one and a small one, namely the Rhône and the Têt, which are discharging to  
8 the Gulf of Lion in the Northwestern Mediterranean Sea. MP fluxes change markedly through time and  
9 space in both river systems. However, no clear relationships between MP concentrations and  
10 hydroclimatic conditions have been observed. In the Rhône River a non-linear dilution pattern of MPs  
11 in total suspended matter (TSM) during flood conditions could be observed. Although dilution is im-  
12 portant, samples during floods exert a strong control on average MP fluxes. Compared to the Rhône  
13 River, average MP concentrations in the Têt River were throughout greater and more variable in shape  
14 and polymer composition. However, as the study year was exceptionally dry, the average specific MP  
15 flux,  $76 \text{ g km}^{-2} \text{ y}^{-1}$ , is only slightly larger than the non-flooding value of the Rhône River. We further  
16 monitored MP concentrations in shoreline sediments at the mouth of the Têt River to test whether these  
17 sediments can represent MP transport in the river. Besides fibers, which probably are easily washed out  
18 and transported offshore, MP concentrations and compositions are in agreement with MP loads up-  
19 stream the river. We also examined the potential role of atmospheric deposition as a source of MP to  
20 the Têt River. The average atmospheric MP deposition of  $6 \text{ kg km}^{-2} \text{ y}^{-1}$  exceeds by far the river average  
21 specific MP flux. Moreover, all MPs in atmospheric deposits were fibers, which in terms of mass are of  
22 minor importance in the bulk river fluxes. Atmospheric MP deposits may either have been overestim-  
23 ated and/or may be removed from surface waters by efficient removal processes (such as waste water  
24 treatment plants).

## 25 **1. Introduction**

26 Terrestrial environments are exposed to a wide variety of pollutants and anthropogenic litter. Among  
27 them, plastics are omnipresent and tend to accumulate within soils, rivers and lakes (e.g. Gang Xu *et*  
28 *al.*, 2006; Gasperi *et al.*, 2014; Faure *et al.*, 2015; Mani *et al.*, 2019; Zhou *et al.*, 2019). Plastics are  
29 resistant, malleable, and degrade slowly. They are nowadays used to make a wide variety of items  
30 (Barnes *et al.*, 2009) and their production and subsequent introduction into the environment have  
31 steadily increased since the middle of the last century (Geyer *et al.*, 2017). These plastic inputs often  
32 result from human negligence, such as inadequate management of waste disposals, urban runoff,  
33 releases from wastewater treatment plants or accidental spills (GESAMP, 2015).

34 Plastics can be separated into different size classes, with macroplastics being larger than 2.5 cm,  
35 mesoplastics ranging between 2.5 cm and 5 mm, microplastics (MPs) ranging between 5 mm and 1  $\mu$ m  
36 and nanoplastics being smaller than 1  $\mu$ m (Cheshire *et al.*, 2009; Lippiatt *et al.*, 2013; MSFD Technical  
37 Subgroup on Marine Litter, 2013). Small plastics come either from the degradation of larger parts or  
38 are directly manufactured in micrometric sizes (e.g. micro-beads or pellets; Barnes *et al.*, 2009). Plastic  
39 debris in the natural environment generate a growing public awareness and concern because they can  
40 be easily ingested by organisms (GESAMP, 2015) and accumulate via the trophic web (Farrell and  
41 Nelson, 2013; Provencher *et al.*, 2018) up to humans (Rochman *et al.*, 2015; Catarino *et al.*, 2018). MP  
42 compounds, monomers and additives, can have deleterious effects on organisms (Lithner *et al.*, 2011;  
43 Rochman *et al.*, 2013; Boots *et al.*, 2019) also because they can adsorb organic pollutants and heavy  
44 metals at their surface (Hirai *et al.*, 2011; Turner and Holmes, 2015; Godoy *et al.*, 2019). MPs have  
45 consequently been proposed as one of ten emerging issues in the UNEP Year Book 2014 and can pose a  
46 potential threat to human health and activities (Eerkes-Medrano *et al.*, 2015; Gasperi *et al.*, 2018).

47 The Mediterranean region is particularly interesting for the study of MP dynamics in the environment.  
48 The coastal waters receive freshwaters from European, Asian and African watersheds. Many of them  
49 host high population densities and the Mediterranean coastline is one of the most popular tourist

50 destinations in the world (UNEP/PAM, 2015). These high anthropogenic pressures combined with an  
51 overall poor waste management capacity lead to high amount of litter dumped into the sea (Schmidt *et*  
52 *al.*, 2017). Its semi-enclosed nature favors litter recirculation and limits its further transfer to other  
53 ocean areas. As a consequence, the Mediterranean Sea is highly exposed to marine litter pollution  
54 (Galgani *et al.*, 1995, 1996; C3zar *et al.*, 2015; Deudero and Alomar, 2015; Tubau *et al.*, 2015; Fossi *et*  
55 *al.*, 2018; Prevenios *et al.*, 2018) and MP concentrations at the sea surface are comparable to those  
56 found in accumulation zones of the large ocean gyres (C3zar *et al.*, 2015).

57 Compared to marine environments, on which most of the public concern on the plastic litter problem is  
58 focused on, knowledge on the distribution and toxicity of MPs in terrestrial environments is poor  
59 (Lambert and Wagner, 2018; Rochman, 2018). This is particularly true for freshwater systems that  
60 receive waters, sediments and various compounds from distant areas and are closely linked to human  
61 activities (Eerkes-Medrano *et al.*, 2015). Some of them, like reservoirs and lakes, act as sinks and  
62 accumulate MPs on their shores, surface waters and bottom sediments (Faure *et al.*, 2015; Ballent *et*  
63 *al.*, 2016; Turner *et al.*, 2019). Others, such as rivers, transport MPs from their headwaters down to the  
64 coastal zone (Moore *et al.*, 2011; Miller *et al.*, 2017). They represent the major pathways of MP  
65 transfer between the atmosphere, land surfaces and aquatic environments, and are suspected to be the  
66 dominant source of MPs to the sea (Lebreton *et al.*, 2017).

67 Only a few studies investigated the transfer of MPs within watersheds discharging into the  
68 Mediterranean Sea (Faure *et al.*, 2015; Schmidt *et al.*, 2018). This study aims to fill this data gap by  
69 carrying out a seasonal MP monitoring in two contrasting river systems of the Gulf of Lion: The Rh3ne  
70 and the T3t rivers. Both rivers are part of the French monitoring observatory MOOSE and are  
71 consequently well documented in terms of their peculiarities for the transfer of water, sediments and  
72 pollutants (e.g., Dumas *et al.*, 2015; Sadaoui *et al.*, 2016). Our main objective was to better understand  
73 the variabilities of concentrations, fluxes, as well as the main shapes and polymeric composition of

74 MPs collected in relation with their potential forcing (precipitation, flow rate, wind regime and specific  
75 events) in order to further foster modelling of the river transfer of MPs to the Mediterranean Sea. In the  
76 case of the Têt River, we completed our approach with two concomitant monitoring points: one on the  
77 atmospheric deposition and the second on sand deposits along the river shore line close to its mouth.  
78 This sampling strategy within the Têt watershed should allow a comparison of MP fluxes between  
79 potential sources (river and atmosphere) and the sink of MPs in the drainage basin (Constant *et al.*,  
80 2017). In the case of the Rhône River, we succeeded sampling during a major flood event, which is  
81 crucial for the establishment of reliable budget calculations for particulate matter transfer in rivers in  
82 general.

## 83 **2. Materials and Methods**

### 84 **2.1. Sampling sites**

85 Samples were collected in two drainage basins (Rhône and Têt rivers) connected to the Gulf of Lion.  
86 The Rhône River is the largest catchment area (about 100,000 km<sup>2</sup>, Tab.1) in western Europe and  
87 nowadays the largest Mediterranean river in terms of freshwater and sediment inputs (Ludwig *et al.*,  
88 2009; Sadaoui *et al.*, 2016). The Têt River on its part is a typical coastal Mediterranean river with a  
89 drainage catchment area lower than 5,000 km<sup>2</sup>. When all coastal Mediterranean rivers inputs are  
90 cumulated, they reach a significant role in the total riverine matter fluxes to the Mediterranean Sea  
91 (Sadaoui *et al.*, 2018). The coastal plain of the Têt watershed is characterized by agricultural activities,  
92 as well as the location of the largest city of the district (Perpignan, about 150,000 inhabitants).  
93 However, population density in the Têt River basin is 1.7 times greater than in the Rhône River basin  
94 (Tab. 1). Population hotspots in the Rhône River basin are situated further upstream and an unknown  
95 fraction of the litter caught by the river basin may be intercepted by one of its 130 dams (Sadaoui *et al.*,  
96 2018). Two major dams exist in the Têt River basin but they lie upstream the densely populated coastal  
97 plains. Both river basins are regularly exposed to strong continental winds (gusts often >100 km h<sup>-1</sup>,

98 called "Mistral" and "Tramontane" winds for the Rhône and Têt plains, respectively) associated with  
99 dry periods. Such intense winds can mobilize sediments from bare grounds and therefore, plastic debris  
100 from dumps and other mismanaged plastic waste sources. These near coast areas are considered to  
101 supply most of the plastic debris to the sea (Jambeck *et al.*, 2015).

102 River surface waters were sampled close to both river mouths (Fig. 1). The sampling station for the  
103 Rhône was at the city of Arles (48 km from the river mouth; 43.678973 N, 4.623029 E), just before the  
104 river splits into two branches entering the Mediterranean Sea separately. The sampling location on the  
105 Têt River was at Sainte-Marie-la-mer (5.5 km from the river mouth; 42.7136938 N, 2.9827452 E)  
106 downstream Perpignan. As the Mediterranean Sea is a microtidal sea, the sampling sites are not  
107 affected by marine intrusion.

108 For MP flux comparison, river shore sediments were taken at the river mouth (42.713048 N, 3.038715  
109 E) and atmospheric deposits were collected in the city of Perpignan (42.683934 N, 2.898160 E) on the  
110 roof of our laboratory (Fig. 1). Perpignan is the main city in the department and concentrates  $\frac{3}{4}$  of the  
111 population in the Têt River basin (Garcia-Esteves *et al.*, 2007).

## 112 **2.2. Sampling strategy**

113 Rivers were sampled using an Oceomic® Manta trawl (60 x 25 cm opening; 333  $\mu$ m mesh) placed at  
114 the top 20 cm of the river surface for 15-60 min periods. Sampled water volumes were recorded with a  
115 mechanical flowmeter (Hydro-bios®; model 438 110) and varied from 32 to 500 m<sup>3</sup> (mean:  $191 \pm 144$   
116 m<sup>3</sup>). Both rivers were sampled during at least one complete hydrological year. Three consecutive  
117 samples were collected every month in the Têt River from December 2015 to October 2016, except the  
118 summer months June, July and August, for which a single sample was taken with a weekly frequency.  
119 The trawl was attached to the central part of a bridge downstream. In total, 35 trawls were carried out at  
120 the Têt River station. Water flow conditions during this sampling period were dryer than on average.  
121 Taking the 2016 year as reference, the mean annual flow rate of the Têt corresponded to only 40% of

122 its long-term mean (about  $10 \text{ m}^3 \text{ s}^{-1}$ , Table 1; Ludwig *et al.*, 2004). This low-flow period has also  
123 strongly impacted the transport of total suspended matter (TSM) in this river. On the basis of the rating  
124 curves published by Sadaoui *et al.* (2016), the averaged TSM flux of the Têt River in 2016 reached  
125 only about 10% of its long-term average (Table 1).

126 Monthly Manta trawl sampling occurred in the Rhône River from October 2015 to October 2016,  
127 resulting in 13 samples. Then, fifteen additional samples were collected with a conical plankton net (10  
128 cm opening radius;  $300 \mu\text{m}$  mesh) from November 2016 to August 2017. This conical net was first  
129 used three consecutive times (5 min long) during a major flood event of the Rhône River ( $5,446 \text{ m}^3 \text{ s}^{-1}$   
130 on the 22<sup>th</sup> November 2016) because of the impossibility to use the large Manta trawl under such strong  
131 flow conditions. Then, from February to July 2017, two conical plankton nets were simultaneously  
132 deployed once a month at the central and the right part of the bridge during 15 min. Filtered water  
133 volumes with the conical plankton net varied from 5 to  $18 \text{ m}^3$  (mean:  $12 \pm 4 \text{ m}^3$ ). Taking the mean  
134 water discharge of the year 2016 as reference (see Tab.1), the Rhône had an average water discharge  
135 close to its long-term mean of about  $1700 \text{ m}^3 \text{ s}^{-1}$  (Ludwig *et al.*, 2009). Using the same method than for  
136 the Têt River, the average TSM flux of the Rhône River in 2016 was estimated to 85% of its long-term  
137 average.

138 Shore sediments at the Têt River mouth were collected at four locations spaced 30 m apart. This  
139 sampling was repeated 8 times from October 2015 to February 2017 with the purpose to obtain samples  
140 before and after rainfall events. The sampling area was delimited by a  $0.5 \times 0.5 \text{ m}$  wood quadrat placed  
141 across the last fresh deposit line. This line corresponds to the last water mark and separates dry and wet  
142 sediments. The top first centimeter of sand was sampled with a steel trowel and sieved through an 8  
143 mm steel sieve placed on top of a metallic funnel to avoid obstruction of the funnel by plant residues  
144 and/or large gravels. The  $<8 \text{ mm}$  fraction was funneled into cleaned glass bottles.

145 Atmospheric deposits were collected using a vertical cylindrical container with similar dimensions  
146 (height: 50 cm; internal diameter: 30 cm; surface: 0.071 m<sup>2</sup>) as the containers used in standard  
147 atmospheric deposition samplers. The container was placed on the flat roof of the laboratory, inside a  
148 higher (90 cm) metallic container to limit air movement and resuspension. In total, 28 samples were  
149 collected at various frequencies (from 5 to 115 days, with a mean of 27 ± 25 days), before and after  
150 rainfall events, from October 2015 to February 2018.

### 151 **2.3. Sample treatments and analysis**

152 Back to the laboratory, the trawl and net were rinsed with a high-pressure hose to recover particles  
153 stuck in the net. Three different treatments were required on the three matrices we analyzed (water,  
154 sediment and atmospheric deposits). In all steps, contamination of the samples was minimized by  
155 wearing laboratory cotton coats, glassware and steel tools. All handling was performed under a laminar  
156 flow hood and beakers were covered by an aluminum foil to protect samples from air contamination. In  
157 most cases, control manipulations that underwent the same treatment than samples were carried out for  
158 the determination of blanks.

159 River samples were transferred from the cod-end trawl collector over a stacked series of 10 mm, 5 mm,  
160 1 mm and 200 µm metal sieves. The contents of the sieve were emptied into glass bottles and sieves  
161 were carefully rinsed with tap water. Then, hydrogen peroxide (H<sub>2</sub>O<sub>2</sub> 40%) was used only when  
162 necessary for removing the remaining biological debris (modified from Faure *et al.*, 2015). During the  
163 entire digestion process, beakers were heated at 50°C on a heating plate. The resulting solutions were  
164 filtered on Whatman® filter papers (47 mm diameter; 2 µm porosity).

165 Sediment samples were also first introduced on a column of sieves (5, 2.5, 1 mm; 500, 315, 63 µm).  
166 MPs were then separated from sediments by flotation in a hypersaline solution (density 1.2 g mL<sup>-1</sup>)  
167 following the widely-used method of Thompson (2004). Extraction of MPs was identical to those  
168 described by Constant *et al.* (2019) in a study on MPs in nearby beach sediments. Samples from

169 atmospheric deposits were transferred from the collector to a glass beaker and then filtered on  
170 Whatman® filter papers according to the method of Dris *et al.* (2016).

171 All filters from river, sediment and atmospheric samples were dried at 50 °C overnight and then  
172 examined under a Wild Heerbrugg dissecting stereo-microscope (6 x, 12 x, 25 x and 50 x  
173 magnification). All suspected MPs were sorted into 5 shape categories: fibers (including filaments and  
174 fishing line fragments), fragments (items with a three-dimensional shape), micro-beads (solid spheres),  
175 films (items with a two-dimensional shape), and foams (pieces or spheres with a spongy, soft structure).  
176 Photos of the different shape categories considered can be found in Constant *et al.* (2019).

177 Finally, **particles longer than 5 mm were sorted out and discarded from counts** all suspected MPs from  
178 each individual sample were weighed together to the nearest 0.01 mg.

179 A total of 370 items was randomly selected and analyzed for polymeric composition (Löder and Gerdts,  
180 2015). 120 fibers (40 fibers per compartment) were analyzed with a microscope IR-Plan Spectra Tech®  
181 coupled to an ABB® FTLA2000 FTIR spectrometer. 130 fragments, 64 films, 44 foams and 12 beads  
182 from river water and shore samples (80-85 items per river basin) were analyzed with a Frontier FTIR  
183 spectrometer (PerkinElmer®). The identification of each polymer was performed by comparison with a  
184 self-collected spectrum database including polyethylene (PE), polypropylene (PP), polyamide (PA),  
185 polyvinyl chloride (PVC), polystyrene (PS), poly(ethylene-vinyl acetate) (PEVA), poly(ethylene  
186 terephthalate) (PET), polyester (PES), polyurethane (PUT), acrylic (A) and some non-plastic materials  
187 such as cotton, wool, wood, paper, calcium carbonate, talcum powder and plant fibers (see details in  
188 Constant *et al.*, 2019).

189 FTIR analysis was used to correct the initial sorting and to accurately determine the true number and  
190 mass of MPs in our samples. For each shape category, an identified plastic ratio was accordingly  
191 applied. This ratio was calculated by dividing the number of true MPs (particles with a “plastic  
192 spectra”) by the total number of sorted items and visually described as “potential plastics”. All MP

193 contents and relative contents of shapes given in the following text, figures and tables are based on true  
194 MPs. Mean values are provided  $\pm$  1 standard error. Fibers in river samples were mostly found gathered  
195 to lint composed of an innumerable amount of tangled fibers. Each lint was weighed to estimate the  
196 number of fibers using the equations of Napper and Thompson (2016). Briefly, the mass of lint was  
197 divided by the theoretical mass of one fiber. Parameters used in this study to calculate the mass of a  
198 single fiber were length, diameter and density. Length (mean: 1.6 mm  $\pm$  0.9 mm) and diameter (mean:  
199 22  $\mu$ m  $\pm$  6  $\mu$ m) were based on 60 measures performed with a stereo-microscope equipped with a  
200 camera (Leica®) and an image treatment software (Leica®). Density was calculated based on FTIR  
201 results and mean weighted density of PES (1.24 g cm<sup>-3</sup>, 70%), A (1.02 g cm<sup>-3</sup>, 20%), PP (0.9 g cm<sup>-3</sup>,  
202 10%). Concentrations of MPs were estimated by dividing the corrected numbers of identified plastic  
203 items and the corrected mass of identified plastic by the volume of filtered water (items and mg per m<sup>-3</sup>  
204 <sup>3</sup>) for river samples, the surface (items and mg per m<sup>-2</sup>) for sediment shore samples, the weight of the  
205 dry sampled sand (items and mg per kg<sup>-1</sup>) for sediment shore or the surface and the sampling interval  
206 (items per m<sup>-2</sup> per day) for atmospheric deposits. Statistical analyses were performed using R software  
207 (see details in Constant *et al.*, 2019).

### 208 **3. Results**

#### 209 **3.1 Riverine MP concentrations, shapes and polymeric composition**

210 MP numerical and mass concentrations were significantly higher in the Têt River than in the Rhône  
211 River for Manta samples (Wilcoxon test, p = 0.05 and p < 0.01, respectively; Figs. 2A and E). Samples  
212 taken at the Rhône River with the Manta trawl and the conical net did not show significant differences  
213 in MP numerical concentrations (Wilcoxon test, p = 0.24; Fig. 2A). However, mass concentrations were  
214 significantly higher with conical nets than Manta trawls (Wilcoxon test, p = 0.03; Fig. 2E).

215 Numerical concentrations of MPs in the Rhône River ranged from 0.3 to 58.9 with a mean of 11.6  $\pm$   
216 17.7 items m<sup>-3</sup> when using the Manta trawl (Figs. 2A and Tab. 2). Mass concentrations ranged from

217 0.007 to 0.6 mg m<sup>-3</sup> with a mean of 0.1 ± 0.2 mg m<sup>-3</sup> (Figs. 2E and Tab. 2). Using the conical plankton  
218 net, MP concentrations ranged from 2.4 to 88.4 items m<sup>-3</sup> with a mean of 18.8 ± 28.1 items m<sup>-3</sup> and  
219 from 0.01 to 3.9 mg m<sup>-3</sup> with a mean of 0.5 ± 1.0 mg m<sup>-3</sup> (Figs. 2A, E and Tab. 2). The position of the  
220 conical net on the bridge (center or right) across the Rhône riverbed did not affect significantly the  
221 numerical and mass concentrations of MPs (paired Wilcoxon test, p = 0.16 and p = 0.44, respectively;  
222 Figs. 2B and F).

223 Three consecutive replicates were performed on the Têt River with a Manta trawl at nine sampling  
224 dates (Figs. 2C and G). Numerical concentrations varied within two orders of magnitude between  
225 replicates and four orders of magnitude over the survey, from 0.8 to 618.5 items m<sup>-3</sup> with a mean of  
226 42.3 ± 107.3 items m<sup>-3</sup> (Tab. 2). Mass concentrations showed much less variability and ranged from  
227 0.02 to 3.4 mg m<sup>-3</sup> with a mean of 0.8 ± 0.8 mg m<sup>-3</sup>.

228 Riverine MPs showed a similar distribution pattern of shapes between the Rhône and Têt rivers (Fig.  
229 3). Whatever the sampling gear used (Manta trawl or conical net), fibers were by far the most abundant  
230 shape (Rhône: 98.0%; Têt: 92.5%), followed by fragments (Rhône: 1.4%; Têt: 4.5%). Foams (Rhône:  
231 0.3%; Têt: 1.2%) and films (Rhône: 0.3%; Têt: 1.1%) were less represented. Micro-beads were  
232 negligible in the Rhône River and slightly more numerous in the Têt River (Rhône: <0.1%; Têt: 0.7%).  
233 Variability of MP shapes was hence greater in the Têt River than in the Rhône River. Despite the large  
234 predominance of fibers in both rivers, they only represented on average 3.6% (Têt) and 6.7% (Rhône)  
235 of all MP masses.

236 Most of binocular-sorted items in river surface waters and considered as "suspected MPs" were  
237 validated as "true MPs" after FTIR control (85%). Fibers in rivers were dominantly made of PES  
238 (63%). A, PP, and non-plastic items were also found (< 15%). Fragments and films were mostly made  
239 of plastics (fragments: Rhône 71%, Têt 92%; films: Rhône 96%, Têt 86%) and composed of PE and PP  
240 (Rhône fragments: 42% PE, 16% PP; Rhône films: 56% PE, 12% PP; Têt fragments: 39% PE, 33% PP;

241 Têt films: 41% PE, 36% PP). Foams were mostly composed of PS (Rhône: 73%; Têt: 87%). All sorted  
242 beads were exclusively made of PE.

### 243 **3.2 Variability of MP concentrations as related to hydroclimatic forcing**

244 Manta trawls in the Rhône River were performed from Oct. 2015 to Oct. 2016 over a large range of  
245 daily flow rates ( $676 - 2,526 \text{ m}^3 \text{ s}^{-1}$ ) and TSM ( $3 - 92 \text{ mg}$  of suspended particles  $\text{L}^{-1}$ ), both ranges being  
246 however clearly below flood levels. Numerical and mass concentrations did not show the same pattern  
247 along the year (Fig. 4). The highest numerical concentration ( $58.9 \text{ items m}^{-3}$ ) at the end of May 2016  
248 occurred during a small rainfall event (4 mm) at Arles and with a flow rate around  $2,000 \text{ m}^3 \text{ s}^{-1}$ . The  
249 highest mass concentration ( $0.6 \text{ mg.m}^{-3}$ ) was recorded at the end of October 2016 during a rainfall  
250 event (16 mm) but a low flow rate ( $936 \text{ m}^3 \text{ s}^{-1}$ ).

251 In November 2016, we changed our sampling strategy with the repeated use of a conical net to sample  
252 high flow rate conditions until July 2017. In conjunction with a local rainfall event of 15 mm, the flow  
253 rate and the TSM concentration of the Rhône River increased to  $8,260 \text{ m}^3 \text{ s}^{-1}$  and  $6,309 \text{ g L}^{-1}$  at the end  
254 of November (Fig.4), indicating a strong flood with a 13-year return period (Sadaoui *et al.*, 2016).  
255 Despite other rainfall events between March and May 2017, flow rates decreased and oscillated  
256 between  $1,000$  and  $2,000 \text{ m}^3 \text{ s}^{-1}$ . Numerical and mass concentrations during the two first sampling dates  
257 with the conical net did not show the same patterns than during the rest of our study period. Highest  
258 numerical concentrations occurred during the flood, whereas the mass concentration peaked in the  
259 beginning of February 2017 during a dry day and with a medium flow rate of  $1,582 \text{ m}^3 \text{ s}^{-1}$ .

260 The sampling period on the Têt River was characterized by few rainfall events  $>10 \text{ mm}$ , mainly  
261 occurring in spring and autumn (Fig. 5), whereas winter and summer were rather dry. The highest  
262 numerical concentration ( $618 \text{ items m}^{-3}$ ), one order of magnitude higher than the other concentrations,  
263 happened in May 2016 during a dry period with a low daily flow rate ( $3 \text{ m}^3 \text{ s}^{-1}$ ; Fig. 6). This high MP  
264 content was not related to a high mass of plastic. The highest mass concentrations were found in one of

265 the triplicates of December 2015 and February 2016 (both at  $3.4 \text{ mg m}^{-3}$ ). Both samples were collected  
266 after a long period of low water levels without precipitation and demonstrate the large variability of  
267 results within triplicates (Fig. 2 G). As for the Rhône River, no clear patterns could hence be observed  
268 between both numerical and mass concentrations of MP and river flow rate, rainfall and TSM  
269 concentrations (Fig. 6). Nevertheless, most trawls in the Têt River were performed during low flow  
270 conditions ( $< 5 \text{ m}^3 \text{ s}^{-1}$ ), which represented 80% of all daily flow rates measured during our 1-yr  
271 sampling period.

### 272 **3.3 Deposition of MP in the Têt River basin**

#### 273 3.3.1 Shoreline sediments

274 Contrary to surface waters, numerical and mass concentrations of MPs in the shore sediments of the  
275 Têt mouth followed a similar pattern. Concomitant samples collected 30 m apart showed a high spatial  
276 heterogeneity that tended to increase with high concentrations (Fig. 5). MP concentrations ranged from  
277 7 to 1,029 items  $\text{kg}^{-1}$  and from 4 to 633  $\text{mg kg}^{-1}$  with means over the sampling period of  $258 \pm 259$   
278 items  $\text{kg}^{-1}$  and  $133 \pm 136 \text{ mg kg}^{-1}$  (Tab. 3). Highest concentrations were found in October 2015 and  
279 September 2016 ( $1,029 \text{ items kg}^{-1}$  and  $708 \text{ mg kg}^{-1}$ ,  $755 \text{ items kg}^{-1}$  and  $257 \text{ mg kg}^{-1}$ , respectively). Both  
280 samples were collected just after a rain event (13 and 14 mm, respectively) which provoked a weak  
281 flow rate increase (to 9 and  $4 \text{ m}^3 \text{ s}^{-1}$ , respectively). Replicates from the end of August 2016, which had  
282 low mean concentrations ( $184 \pm 110 \text{ items kg}^{-1}$  and  $94 \pm 60 \text{ mg kg}^{-1}$ ), have been collected after a long  
283 period of low water stage without precipitation. The lowest mean concentrations of December 2016  
284 and February 2017 ( $44 \pm 52 \text{ items kg}^{-1}$  and  $26 \pm 30 \text{ mg kg}^{-1}$ ,  $24 \pm 19 \text{ items kg}^{-1}$  and  $16 \pm 13 \text{ mg kg}^{-1}$ ,  
285 respectively) were both taken a few days after an important rain event (7 and 59 mm, respectively),  
286 which also provoked peaks in the river flow rates ( $56$  and  $87 \text{ m}^3 \text{ s}^{-1}$ , respectively).

287 Shapes and polymers in shore sediments of the Têt mouth were different compared to the river surface  
288 waters (Fig. 3). Fragments were the most abundant shape (54.8%), followed by fibers (19.5%), foams  
289 (13.0%), films (7.0%) and beads (5.7%). Most of binocular-sorted items in shore sediments (79%) were

290 plastic, but 40% of fibers were non plastic. Among the plastic fibers, PES, PP, PA and A were  
291 identified. Fragments and films were mostly plastic (82% and 76%, respectively) and composed of PE  
292 and PP (fragments: 45% PE, 23% PP; films 29% PP, 35% PP). Half of foams were composed of PS and  
293 all beads were made of PE.

### 294 3.3.2 Atmospheric fallout

295 MP concentrations in atmospheric deposits at Perpignan ranged from 5 to 65 items  $\text{m}^{-2} \text{d}^{-1}$  with a mean  
296 of  $22 \pm 14$  items  $\text{m}^{-2} \text{d}^{-1}$  (Fig. 7; Tab. 3). During the two sampling years (790 days), 75% of days were  
297 dry and the average daily precipitation was 4 mm per rain event. Only 20 events surpassed 10 mm and  
298 the maximum value of 54 mm was recorded at the end of March 2017 (Fig. 7). Winds with a mean  
299 velocity of  $9 \text{ m s}^{-1}$  originated half of the time from the NNW (continental and dry wind, see details in  
300 section 2.1), and for 20% from E (moist wind). For 49 days, the intense and dry NNW wind blew with  
301 a daily mean velocity greater than  $15 \text{ m s}^{-1}$ . The peak of 65 items  $\text{m}^{-2} \text{d}^{-1}$  occurred in April 2017 during  
302 a rainfall event of 6 mm. The April 2017 sample (11 items  $\text{m}^{-2} \text{d}^{-1}$ ) was the single sample only  
303 associated with dry deposits. When cumulated rainfall of the sampling period was at its maximum (178  
304 mm between December 2016 and February 2017), the MP concentration reached an intermediate value  
305 with 21 items  $\text{m}^{-2} \text{d}^{-1}$ . As in both studied rivers, no clear patterns were found during the sampling period  
306 between MP concentrations in atmospheric fallout and cumulated precipitation (Fig. 6), nor with mean  
307 wind velocity.

308 Fibers were the only shape found in atmospheric deposits (Fig. 3). Most of the suspected fibers (67.5%)  
309 were non-plastic. Such a low percentage of validated plastic fibers illustrates the difficulty in  
310 discriminating plastic fibers from cotton and plant fibers with a binocular or a dissecting stereo-  
311 microscope. Polymers of fibers are in a descending order made of PES, PP, PA and A.

## 312 **4. Discussion**

### 313 **4.1 Export fluxes of MP by the Rhône and Têt rivers**

314 The establishment of reliable MP fluxes from river basins to the sea is one of the major challenges for  
315 our understanding of cycling and impact of plastic litter in the marine environment. This is particularly  
316 true for the Mediterranean Sea, which has been identified as a hotspot region for MP accumulation in  
317 surface waters (Cózar *et al.*, 2015) and which is strongly influenced by its surrounding drainage basins  
318 (Ludwig *et al.*, 2009). It is only very recently that a few pioneering studies proposed general modelling  
319 approaches to quantify these fluxes (Lebreton *et al.*, 2017; Schmidt *et al.*, 2017). However, they are  
320 based on relatively few field observations and Mediterranean rivers are under-represented in these  
321 studies. A major problem for the development of general budget calculations is the great spatial and  
322 temporal variabilities of MP concentrations in river samples, which complicate the definition of  
323 representative levels based on isolated sampling. Our results clearly confirm this variability. Only long-  
324 term monitoring, which contributes to the identification of the major controls on MP fluxes in rivers,  
325 can reduce uncertainties in this respect.

326 Methodological problems contribute also to the difficulties in the determination of representative flux-  
327 es. Manta nets are frequently used for the collection of MPs in rivers, in analogy to studies on MPs in  
328 seawater. Since Manta nets cannot be deployed in rivers during flood conditions, due to a high risk of  
329 deterioration or loss, measurements refer to low flow conditions, which are representative of a typical  
330 hydrological year but not of annual water and sediment budgets. In our river samples (both Rhône and  
331 Têt), no clear relationships were found between MP concentration patterns and those of external factors  
332 such as precipitation, flow rate, and TSM concentrations (Fig. 6). Nevertheless, Figure 8 shows that the  
333 pool of MP within TSM does not decrease linearly with the increase of TSM concentration, as it is fre-  
334 quently found in rivers for other particulate compounds, such as particulate organic carbon (Ludwig  
335 and Probst, 1996; Higuera *et al.*, 2014). In other words, there is a dilution of MP within TSM in both

336 rivers, but the dilution is lower than expected at the highest TSM concentration (flood events). The  
337 dilution is consequently not only the result of the increasing TSM concentrations since flood samples  
338 are somewhat enriched in MPs compared to what might be expected from dilution alone. In addition,  
339 this dilution is not only visible in the Rhône River where we could sample a wider range of TSM con-  
340 centrations, but also in the Têt River, despite the narrower range of TSM concentrations. Data points of  
341 the Têt River are mostly plotted above the data points for the Rhône which is consistent with the great-  
342 er MP concentrations we observed for this river compared to the Rhône River. Figure 8 also indicates  
343 that there is no fundamental difference between the use of a Manta trawl (330 $\mu$ m, 0.15 m<sup>2</sup>) and a coni-  
344 cal net (300 $\mu$ m, 0.03 m<sup>2</sup>). All data points could consequently be used for calculation of the average MP  
345 fluxes in both rivers during the study period.

346 When only referring to samples collected with a Manta net (n=13 for the Rhône River and n=35 for the  
347 Têt River), we obtain arithmetic averages of MP mass concentrations of 0.121 mg m<sup>-3</sup> for the Rhône  
348 and 0.831 mg m<sup>-3</sup> for the Têt. Weighting each concentration with the corresponding TSM  
349 concentrations, in order to better consider hydrological condition, only slightly modify mean values to  
350 0.111 mg m<sup>-3</sup> and 0.828 mg m<sup>-3</sup>, respectively, probably due to the narrow range of TSM concentrations.  
351 Multiplying these concentrations by the 2016 average water discharges yields mean annual MP fluxes  
352 of 5.92 and 0.09 t yr<sup>-1</sup> for the Rhône and Têt rivers, respectively. Then, dividing them by the  
353 corresponding basin areas, yields specific MP fluxes of 61 (Rhône) and 76 g km<sup>-2</sup> (Têt). However,  
354 when we include samples from the Rhône River performed with a conical net (increasing the total  
355 samples to n= 28), the average TSM-weighted MP concentration for the Rhône increases to 0.404 mg  
356 m<sup>-3</sup>, and therefore, the simple and specific MP fluxes become 22 t yr<sup>-1</sup> and 224 g km<sup>-2</sup>, *i.e.* 3-4 times the  
357 previous values. These results clearly demonstrate that "flood" samples collected with the small conical  
358 net have a dominant role in the calculation of realistic MP fluxes in rivers

## 359 **4.2 Comparison with other European watersheds**

360 Sampling methods and treatments vary substantially between the different studies on MPs in aquatic  
361 environments (Hidalgo-Ruz *et al.*, 2012). In Europe, surface water samples were generally taken with  
362 nets of 80 to 800  $\mu\text{m}$  mesh size, including the Manta trawl, stationary conical nets and driftnets. Other  
363 devices such as glass jars, Niskin bottles, continuous centrifugation systems and motor water pumps  
364 have been used (Lechner *et al.*, 2014; Dris *et al.*, 2015; Faure *et al.*, 2015; Mani *et al.*, 2015; Leslie *et*  
365 *al.*, 2016; Rodrigues *et al.*, 2018; Schmidt *et al.*, 2018). All studies sorted MPs visually with a stereo-  
366 microscope and results are dependent on observer abilities. Comparison between studies are therefore  
367 quite difficult to achieve, and only studies using a similar sampling device (net with  $>300 \mu\text{m}$  mesh)  
368 are discussed thereafter.

369 Individual numerical MP concentrations in the Rhône and Têt rivers varied within the range of MP  
370 concentrations measured in other European rivers, but average concentrations were greater by one to  
371 two orders of magnitude (Tab. 4). This shift is likely due to fibers. They represented the dominant  
372 shape in our samples ( $>92.5\%$ ), but they only accounted for 2.5% in the Rhine River (Mani *et al.*,  
373 2015) and 10% in the upstream part of the Rhône River (Faure *et al.*, 2015). Dris *et al.* (2015) for the  
374 Seine River and Lechner *et al.* (2014) for the Danube River did not mention any fiber percentages.  
375 Fibers were also excluded by Schmidt *et al.* (2018) in their study on the Rhône River at Arles. Without  
376 fibers, our mean MP concentrations (Rhône net:  $1.4 \pm 1.1 \text{ items m}^{-3}$ ; Rhône Manta:  $0.3 \pm 0.2 \text{ items m}^{-3}$ ;  
377 Têt Manta:  $1.8 \pm 1.3 \text{ items m}^{-3}$ ) perfectly match values found in the Danube, Seine and upper Rhône  
378 rivers but remain lower compared to the Rhine River where fibers were almost negligible. In all cases  
379 however plastic fibers have to be considered to provide accurate worldwide assessments of the MP  
380 pollution.

## 381 **4.3 Trapping of MPs in the Têt River bank sediments**

382 River bank sediments are transitory sinks for particulate material transported by river waters and  
383 provisory deposited there due to the reduction of flow energy. One can therefore reasonably question

384 the possible role that these sediments, especially those at or nearby river mouths, could play as  
385 indicators of the nature and/or quantity of MPs transported by rivers before they enter the sea. This  
386 could be particularly helpful since shore sediments are easier to sample and theoretically less prone to  
387 short temporal changes than surface waters. Since riparian sediments undergo grain size sorting once  
388 deposited, they are not necessarily representative of the riverine transport in general and direct  
389 comparison should be done with caution. They are mainly composed of sand, contrary to river  
390 sediments in transit that are largely dominated by finer grain size fractions. It can nevertheless be  
391 supposed that trapping efficiency of riverine MP, with the noticeable exception of fibers, may be  
392 comparable to the trapping efficiency of riverine sand. They are relatively coarse in size preventing  
393 them to be backwashed to the river through water percolation in the sediments. A rough budget  
394 calculation can thus be based on the assumptions that the mass ratios of MP to sand in riparian  
395 sediments and in TSM are similar and that the average MP concentration of  $133 \text{ mg kg}^{-1}$  in the Têt river  
396 bank sediments might be representative for the transport of the sand fraction in general. During 2016,  
397 the Têt River transported about 4,500 t of TSM with an average 20% of sand (unpublished results).  
398 This would correspond to an overall riverine MP flux of  $0.12 \text{ t yr}^{-1}$ , close to the MP flux of  $0.09 \text{ t yr}^{-1}$  or  
399  $76 \text{ g km}^{-2}$  calculated above (see section 4.1). The similarity between the two independent estimates is  
400 striking and in favor of using river bank sediments as a convenient, first-order indicator of riverine  
401 MPs.

402 Regarding the quality of MPs, shapes differed markedly between the Têt surface waters (93% of fibers)  
403 and the river bank sediments at its mouth (only 20%). Fibers did not likely settle along the shore but  
404 they might have been washed to the sea before sedimentation. As fibers only weakly contributed to the  
405 mass concentration of MPs in the Têt River (4%), this difference in the MP shapes should only be of  
406 minor importance for MP mass fluxes. PE and PP fragments in both river surface waters and shore  
407 sediments were the dominant plastic polymers with about the same relative proportions (Fig. 3). This

408 result suggests that MP deposits at the shoreline are roughly representative of the coarser MPs  
409 transported by the Têt River.

410 MP concentrations in sediments of the Têt River shore were highly variable along the year. No seasonal  
411 trends were observed and no clear relationship between MP accumulation in shore sediments and MPs  
412 floating in river waters could be detected (Fig. 5). Both parameters could be however closely linked, as  
413 MPs in the shore sediments of the mouth may be accumulated for long periods of low water levels.  
414 Indeed, MP concentrations in shore sediments were higher after dry periods and rainfall events that  
415 were not followed by concomitant increases of the water flow rate. A stable height of the river is  
416 probably needed for accumulation of MPs at the sediment and water interface. Moderate and short  
417 precipitation can still increase accumulation by either leaching MPs from the upper part of the shore or  
418 by increasing MP concentrations in the river. Conversely, peaks in flow rate provoke lower  
419 concentrations. An increase of flow rate increases the river height and may either deposit MPs on the  
420 upper parts of the shore or wash them back to the river in the lower parts.

421 In Europe, only few studies investigated MPs in river shore sediments (Klein *et al.*, 2015; Scheurer and  
422 Bigalke, 2018; Blair *et al.*, 2019) using a similar methodology (surface samples, NaCl gravity  
423 separation, oxidation of natural debris and FTIR verification). Klein *et al.* (2015) monitored shores  
424 along the Rhine and one of its major tributaries, the Main River, at a larger (~40 km) spatial scale than  
425 we did and with only a single sampling period. No mean values were given, but the highest MP  
426 concentrations (Tab. 3) they provided indicate that Rhine River shores are probably more contaminated  
427 than the Têt River shore. This is consistent with the greater population densities in this area (according  
428 to the authors, 300-2900 inhabitant km<sup>-2</sup> for the Rhine and Main watersheds). They also reported  
429 fragments and fibers as the dominant MP compounds in their samples. Scheurer and Bigalke (2018)  
430 found microplastics in 90% of the 29 floodplain soils analyzed across Switzerland, with concentrations  
431 ranging from 0 and 593 MPs kg<sup>-1</sup>, correlated with the population of the catchment. Blair *et al.* (2019)

432 observed 161 and 432 MPs  $\text{kg}^{-1}$  within two samples along the River Kelvin in Glasgow (UK), with  
433 fibers as the dominant shape (> 88%).

#### 434 **4.4 Atmospheric deposits of MP in the Têt River basin**

435 Atmospheric deposits represent a potential source of MPs in rivers. They can enter the aquatic  
436 environment after being washed off from the ground during rainy periods or directly by wind transport.  
437 However, connecting atmospheric MP fallout and MPs in rivers is a difficult task with the available  
438 data. Taking an average deposition rate of 22 fibers  $\text{m}^{-2} \text{d}^{-1}$  converted into mass fluxes on the basis of  
439 the conversion factor for fibers ( $0.7 \mu\text{g fiber}^{-1}$ ; see section 2.3 for details), the only MP shape in our  
440 atmospheric deposits, we determined a fiber deposition rate of  $6 \text{ kg km}^{-2} \text{ yr}^{-1}$ , which is closed to the  
441 estimation made for the Parisian agglomeration ( $1\text{-}4 \text{ kg km}^{-2} \text{ yr}^{-1}$ ; Dris *et al.*, 2016), but two order of  
442 magnitude higher than the mean specific MP flux ( $0.07 \text{ kg km}^{-2} \text{ yr}^{-1}$ ) of the Têt River. Even assuming  
443 that our deposition rate is only valid for the urban area of Perpignan (about 5% of the Têt drainage  
444 basin area) and that no MPs were emitted within natural and agricultural areas, the MP mass flux of  
445 atmospheric deposition would still surpass the river export by a factor of almost 4. In addition, as fibers  
446 only represent a minor part (4%) of the MP mass flux in the Têt River, the difference is even more  
447 important when considering only this shape. Simple mass balance calculations have hence to be done  
448 with caution. Considerable parts of surface water discharge in urban areas pass through waste-water  
449 treatment plants (WWTP), which, according to Murphy *et al.* (2016), can retain up to 98% of MPs.  
450 Moreover, one has also to keep in mind that atmospheric deposition rates of fibers are difficult to  
451 determine with traps, as the same fibers might be remobilized several times by winds. The deposition  
452 rate given here is probably overestimated.

453 Comparing atmospheric MP deposition and riverine MP export is nevertheless interesting for two  
454 reasons. First, it has to be noticed that only fibers (100%) were present in our atmospheric samples,  
455 while the other MP shapes represented 96% of the mean MP mass flux in the Têt River. In other words,

456 riverine MPs have been essentially mobilized through overland water flow and not through  
457 atmospheric deposition. On the other hand, our results suggest that atmospheric transport of MP fibers  
458 could be order(s) of magnitude higher than riverine transport. Direct atmospheric fallout might  
459 potentially represent an important source of MPs entering the sea, especially along the Mediterranean  
460 coast where several continental and intense winds are recorded (*e.g.* Tramontane, Mistral, Bora,  
461 Etesian, Meltemi and Sirocco winds). Further studies should focus more precisely on the quantification  
462 and distribution of MPs in atmospheric deposition along the Mediterranean coast.

463 Dris *et al.* (2016) and Cai *et al.* (2017) investigated atmospheric fallout at two and three urban sites in  
464 Paris (France) and Dongguan city (China), respectively. In both studies, corrected numerical  
465 concentrations (without non plastic items) of MPs were similar to what we found in our study, with  $15$   
466  $\pm 11$  and  $32 \pm 28$  items  $\text{m}^{-2} \text{day}^{-1}$  for Paris (plastic ratio: 0.29; Dris *et al.*, 2016) and  $36 \pm 7$  items  $\text{m}^{-2}$   
467  $\text{day}^{-1}$  for Dongguan city (plastic ratio: 0.16; Cai *et al.*, 2017; see Tab. 3 for uncorrected values). Both  
468 studies also confirm that fibers are the main particle shape in atmospheric MPs and that only about  
469 25% of the suspected plastic fibers are made of plastics. Klein and Fischer (2019) investigated three  
470 urban and three rural sites in the metropolitan region of Hamburg (Germany). Median abundance  
471 ranged between 136.5 and 512.0 items  $\text{m}^{-2} \text{day}^{-1}$  and most of their particles were fragments smaller than  
472  $63 \mu\text{m}$  which is below our detection limit ( $100\mu\text{m}$ ) and the detection limits of previous studies. Allen *et*  
473 *al.* (2019) showed the direct atmospheric fallout of MPs in a remote area of the Pyrenees Mountains,  
474 with an average flux of  $365 \pm 69$  items  $\text{m}^{-2} \text{d}^{-1}$ . Most of their particles were fragments smaller than  $50$   
475  $\mu\text{m}$ .

476 MP concentrations, in our atmospheric fallout samples, were highly variable. Deposition rate did not  
477 show any relationship with neither precipitation nor wind velocity during the sampling periods (Fig. 6  
478 and 7). Dris *et al.* (2016) also observed highly variable levels of MPs within atmospheric fallout of the  
479 Parisian agglomeration, with no significant correlation with mean daily rainfall.

## 480 **5. Conclusions**

481 This study was designed to investigate the contamination by microplastics (MPs) in rivers and  
482 atmospheric fallout. Three environmental matrices (water, sediment, atmosphere) were sampled  
483 monthly during, at least, one year. The conclusions drawn are supported by the results obtained within  
484 two contrasting river systems opening into the Gulf of Lion, a large one (Rhône River) and a small one  
485 (Têt River). These are the following:

486 (1) Relationships between concentrations, fluxes and potential hydroclimatic forcing parameters are  
487 difficult to establish under regular conditions (*i.e.* without extreme events). However, our flood sam-  
488 ples suggest a strong contribution of floods to total MP fluxes.

489 (2) In terms of concentration by the number, fibers are the dominant shape within surface river samples  
490 (>90%). However, in terms of mass concentrations, fibers are only a minor part of riverine MP fluxes  
491 (Rhône: 2%; Têt: 4%). Specific conversion factors of numerical concentrations to mass concentrations  
492 should therefore be applied to each shape category.

493 (3) MP average concentrations, shape and polymer compositions within river bank sediments are con-  
494 sistent with their riverine counterparts, except for fibers that might be easily washed further offshore.  
495 Shoreline sediments nearby river mouths could therefore be informative regarding MP pollution levels  
496 in rivers.

497 (4) In the Têt River basin, MPs within atmospheric fallout is exclusively composed by fibers. Atmos-  
498 pheric deposition rates largely exceed riverine export fluxes, suggesting that atmospheric transport of  
499 microplastic fibers to the sea is potentially significant.

## 500 **6. Acknowledgement**

501 We acknowledge the "Ecole Doctorale ED305" from the University of Perpignan Via Domitia for  
502 funding the PhD grant of Mel Constant. We thank Núria Ferrer from the "Centres Científics i  
503 Tecnològics" of the University of Barcelona for her technical support during FTIR analyses. We are

504 also grateful to “Météo–France” for the access to weather data and the Banque Hydro hosted by the  
505 “French Ministère de l'Environnement et du Développement durable” for hydrological data. This re-  
506 search has also been supported by a Catalan Government Grups de Recerca Consolidats grant (2014  
507 SGR 1068). The authors thank the two anonymous reviewers for their helpful comments and valuable  
508 advices.

## 509 **7. References**

- 510 Allen, S., Allen, D., Phoenix, V.R., Roux, G.L., Jiménez, P.D., Simonneau, A., Binet, S., Galop, D., 2019. At-  
511 mospheric transport and deposition of microplastics in a remote mountain catchment. *Nat. Geosci.* 1.  
512 <https://doi.org/10.1038/s41561-019-0335-5>
- 513 Ballent, A., Corcoran, P.L., Madden, O., Helm, P.A., Longstaffe, F.J., 2016. Sources and sinks of microplastics  
514 in Canadian Lake Ontario nearshore, tributary and beach sediments. *Mar. Pollut. Bull.* 110, 383–395.  
515 <https://doi.org/10.1016/j.marpolbul.2016.06.037>
- 516 Barnes, D.K.A., Galgani, F., Thompson, R.C., Barlaz, M., 2009. Accumulation and fragmentation of plastic  
517 debris in global environments. *Philos. Trans. R. Soc. B Biol. Sci.* 364, 1985–1998.  
518 <https://doi.org/10.1098/rstb.2008.0205>
- 519 Blair, R.M., Waldron, S., Phoenix, V.R., Gauchotte-Lindsay, C., 2019. Microscopy and Elemental Analysis  
520 Characterisation of Microplastics in Sediment of a Freshwater Urban River in Scotland, UK. *Environ.*  
521 *Sci. Pollut. Res.* 26, 12491–504. <https://doi.org/10.1007/s11356-019-04678-1>.
- 522 Boots, B., Russell, C.W., Green, D.S., 2019. Effects of Microplastics in Soil Ecosystems: Above and Below  
523 Ground. *Environ. Sci. Technol.* 53, 11496–11506. <https://doi.org/10.1021/acs.est.9b03304>
- 524 Cai, L., Wang, J., Peng, J., Tan, Z., Zhan, Z., Tan, X., Chen, Q., 2017. Characteristic of microplastics in the at-  
525 mospheric fallout from Dongguan city, China: preliminary research and first evidence. *Environ. Sci.*  
526 *Pollut. Res.* 24, 24928–24935. <https://doi.org/10.1007/s11356-017-0116-x>
- 527 Catarino, A.I., Macchia, V., Sanderson, W.G., Thompson, R.C., Henry, T.B., 2018. Low levels of microplastics  
528 (MP) in wild mussels indicate that MP ingestion by humans is minimal compared to exposure via  
529 household fibres fallout during a meal. *Environmental Pollution* 237, 675–684.  
530 <https://doi.org/10.1016/j.envpol.2018.02.069>
- 531 Cheshire, A. C., Adler, E., Barbière, J., Cohen, Y., Evans, S., Jarayabhand, S., Jeftic, L., Jung, R. T., Kinsey, S.,  
532 Kusui, E. T., Lavine, I., Manyara, P., Oosterbaan, L., Pereira, M. A., Sheavly, S., Tkalin, A., Varadarajan,  
533 S., Weneker, B. and Westphalen, G., 2009. UNEP/IOC guidelines on survey and monitoring of marine  
534 litter. UNEP Regional Seas Reports and Studies No. 186, IOC Technical Series No. 83, 120 p.
- 535 Constant, M., Kerhervé, P., Heussner, S., 2017. Source, Transfer, and Fate of Microplastics in the Northwestern  
536 Mediterranean Sea: A Holistic Approach, in: Baztan, J., Jorgensen, B., Pahl, S., Thompson, R.C.,  
537 Vanderlinden, J.-P. (Eds.), *Fate and Impact of Microplastics in Marine Ecosystems*. Elsevier, pp. 115–  
538 116.

- 539 Constant, M., Kerhervé, P., Mino-Vercellio-Verollet, M., Dumontier, M., Sánchez Vidal, A., Canals, M.,  
540 Heussner, S., 2019. Beached microplastics in the Northwestern Mediterranean Sea. *Mar. Pollut. Bull.*  
541 142, 263–273. <https://doi.org/10.1016/j.marpolbul.2019.03.032>
- 542 Constant, M., Kerherve, P., Sola, J., Sanchez-Vidal, A., Canals, M., Heussner, S., 2018. Floating Microplastics  
543 in the Northwestern Mediterranean Sea: Temporal and Spatial Heterogeneities, in: Cocca, M., Di Pace,  
544 E., Errico, M.E., Gentile, G., Montarsolo, A., Mossotti, R. (Eds.), *Proceedings of the International Con-*  
545 *ference on Microplastic Pollution in the Mediterranean Sea*. Springer International Publishing, Cham,  
546 pp. 9–15.
- 547 Cózar, A., Sanz-Martín, M., Martí, E., González-Gordillo, J.I., Ubeda, B., Gálvez, J.Á., Irigoien, X., Duarte,  
548 C.M., 2015. Plastic accumulation in the Mediterranean Sea. *PLoS One* 10, e0121762.
- 549 Dehghani, S., Moore, F., Akhbarizadeh, R., 2017. Microplastic pollution in deposited urban dust, Tehran metro-  
550 polis, Iran. *Environ. Sci. Pollut. Res.* 1–12. <https://doi.org/10.1007/s11356-017-9674-1>
- 551 Deudero, S., Alomar, C., 2015. Mediterranean marine biodiversity under threat: Reviewing influence of marine  
552 litter on species. *Mar. Pollut. Bull.* 98, 58–68. <https://doi.org/10.1016/j.marpolbul.2015.07.012>
- 553 Dris, R., Gasperi, J., Rocher, V., Saad, M., Renault, N., Tassin, B., 2015. Microplastic contamination in an urban  
554 area: a case study in Greater Paris. *Environ. Chem.* 12, 592. <https://doi.org/10.1071/EN14167>
- 555 Dris, R., Gasperi, J., Saad, M., Mirande, C., Tassin, B., 2016. Synthetic fibers in atmospheric fallout: A source of  
556 microplastics in the environment? *Mar. Pollut. Bull.* 104, 290–293.  
557 <https://doi.org/10.1016/j.marpolbul.2016.01.006>
- 558 Dumas, C., Ludwig, W., Aubert, D., Eyrolle, F., Raimbault, P., Gueneugues, A., Sotin, C., 2015. Riverine trans-  
559 fer of anthropogenic and natural trace metals to the Gulf of Lions (NW Mediterranean Sea). *Appl.*  
560 *Geochem.* 58, 14–25. <https://doi.org/10.1016/j.apgeochem.2015.02.017>
- 561 Eerkes-Medrano, D., Thompson, R.C., Aldridge, D.C., 2015. Microplastics in freshwater systems: A review of  
562 the emerging threats, identification of knowledge gaps and prioritisation of research needs. *Water Res.*  
563 75, 63–82. <https://doi.org/10.1016/j.watres.2015.02.012>
- 564 Farrell, P., Nelson, K., 2013. Trophic level transfer of microplastic: *Mytilus edulis* (L.) to *Carcinus maenas* (L.).  
565 *Environ. Pollut.* 177, 1–3. <https://doi.org/10.1016/j.envpol.2013.01.046>
- 566 Faure, F., Demars, C., Wieser, O., Kunz, M., de Alencastro, L.F., 2015. Plastic pollution in Swiss surface waters:  
567 nature and concentrations, interaction with pollutants. *Environ. Chem.* 12, 582–591.
- 568 Fossi, M.C., Pedà, C., Compa, M., Tsangaris, C., Alomar, C., Claro, F., Ioakeimidis, C., Galgani, F., Hema, T.,  
569 Deudero, S., Romeo, T., Battaglia, P., Andaloro, F., Caliani, I., Casini, S., Panti, C., Bainsi, M., 2018.  
570 Bioindicators for monitoring marine litter ingestion and its impacts on Mediterranean biodiversity. *Envi-*  
571 *ron. Pollut.* 237, 1023–1040. <https://doi.org/10.1016/j.envpol.2017.11.019>
- 572 Galgani, F., Jaunet, S., Campillo, A., Guenegen, X., His, E., 1995. Distribution and abundance of debris on the  
573 continental shelf of the north-western Mediterranean Sea. *Mar. Pollut. Bull.* 30, 713–717.  
574 [https://doi.org/10.1016/0025-326X\(95\)00055-R](https://doi.org/10.1016/0025-326X(95)00055-R)
- 575 Galgani, F., Souplet, A., Cadiou, Y., 1996. Accumulation of debris on the deep sea floor off the French Mediter-  
576 ranean coast. *Mar. Ecol. Prog. Ser.* 142, 225–234. <https://doi.org/10.3354/meps142225>

- 577 Gang Xu, Qunhui Wang, Qingbao Gu, Yunzhe Cao, Xiaoming Du, Fasheng Li, 2006. Contamination Character-  
578 istics and Degradation Behavior of Low-Density Polyethylene Film Residues in Typical Farmland Soils  
579 of China. *J. Environ. Sci. Health Part B -- Pestic. Food Contam. Agric. Wastes* 41, 189–199.  
580 <https://doi.org/10.1080/03601230500365069>
- 581 Gao, F., Li, J., Sun, C., Zhang, L., Jiang, F., Cao, W., Zheng, L., 2019. Study on the capability and characteris-  
582 tics of heavy metals enriched on microplastics in marine environment. *Marine Pollution Bulletin* 144,  
583 61–67. <https://doi.org/10.1016/j.marpolbul.2019.04.039>
- 584 Garcia-Esteves, J., Ludwig, W., Kerherve, P., Probst, J.L., Lespinas, F., 2007. Predicting the impact of land use  
585 on the major element and nutrient fluxes in coastal Mediterranean rivers: the case of the Têt River  
586 (Southern France). *Appl. Geochem.* 22, 230–248.
- 587 Gasperi, J., Dris, R., Bonin, T., Rocher, V., Tassin, B., 2014. Assessment of floating plastic debris in surface  
588 water along the Seine River. *Environ. Pollut.* 195, 163–166.  
589 <https://doi.org/10.1016/j.envpol.2014.09.001>
- 590 Gasperi, J., Wright, S.L., Dris, R., Collard, F., Mandin, C., Guerrouache, M., Langlois, V., Kelly, F.J., Tassin,  
591 B., 2018. Microplastics in air: Are we breathing it in? *Current Opinion in Environmental Science &*  
592 *Health, Micro and Nanoplastics* Edited by Dr. Teresa A.P. Rocha-Santos 1, 1–5.  
593 <https://doi.org/10.1016/j.coesh.2017.10.002>
- 594 GESAMP, 2015. Sources, Fate and Effects of Microplastics in the Marine Environment: A Global Assessment.
- 595 Geyer, R., Jambeck, J.R., Law, K.L., 2017. Production, use, and fate of all plastics ever made. *Sci. Adv.* 3,  
596 e1700782. Klein, M., Fischer, E.K., 2019. Microplastic Abundance in Atmospheric Deposition within the  
597 Metropolitan Area of Hamburg, Germany. *Sci. Total Environ.* 685, 96–103.  
598 <https://doi.org/10.1016/j.scitotenv.2019.05.405>
- 599 Hidalgo-Ruz, V., Gutow, L., Thompson, R.C., Thiel, M., 2012. Microplastics in the Marine Environment: A  
600 Review of the Methods Used for Identification and Quantification. *Environ. Sci. Technol.* 46, 3060–  
601 3075. <https://doi.org/10.1021/es2031505>
- 602 Hirai, H., Takada, H., Ogata, Y., Yamashita, R., Mizukawa, K., Saha, M., Kwan, C., Moore, C., Gray, H.,  
603 Laursen, D., Zettler, E.R., Farrington, J.W., Reddy, C.M., Peacock, E.E., Ward, M.W., 2011. Organic  
604 micropollutants in marine plastics debris from the open ocean and remote and urban beaches. *Mar.*  
605 *Pollut. Bull.* 62, 1683–1692. <https://doi.org/10.1016/j.marpolbul.2011.06.004>
- 606 Jambeck, J.R., Geyer, R., Wilcox, C., Siegler, T.R., Perryman, M., Andrady, A., Narayan, R., Law, K.L., 2015.  
607 Plastic waste inputs from land into the ocean. *Science* 347, 768–771.  
608 <https://doi.org/10.1126/science.1260352>
- 609 Klein, S., Worch, E., Knepper, T.P., 2015. Occurrence and Spatial Distribution of Microplastics in River Shore  
610 Sediments of the Rhine-Main Area in Germany. *Environ. Sci. Technol.* 49, 6070–6076.  
611 <https://doi.org/10.1021/acs.est.5b00492>
- 612 Lambert, S., Wagner, M., 2018. Microplastics Are Contaminants of Emerging Concern in Freshwater Environ-  
613 nments: An Overview, in: *Freshwater Microplastics, The Handbook of Environmental Chemistry.*  
614 Springer, Cham, pp. 1–23.

- 615 Lebreton, L.C.M., van der Zwet, J., Damsteeg, J.-W., Slat, B., Andrady, A., Reisser, J., 2017. River plastic emis-  
616 sions to the world's oceans. *Nat. Commun.* 8, 15611. <https://doi.org/10.1038/ncomms15611>
- 617 Lechner, A., Keckeis, H., Lumesberger-Loisl, F., Zens, B., Krusch, R., Tritthart, M., Glas, M., Schludermann,  
618 E., 2014. The Danube so colourful: A potpourri of plastic litter outnumbers fish larvae in Europe's se-  
619 cond largest river. *Environ. Pollut.* 188, 177–181. <https://doi.org/10.1016/j.envpol.2014.02.006>
- 620 Leslie, H.A., Brandsma, S.H., van Velzen, M.J.M., Vethaak, A.D., 2016. Microplastics en route: Field measure-  
621 ments in the Dutch river delta and Amsterdam canals, wastewater treatment plants, North Sea sediments  
622 and biota. *Environ. Int.* <https://doi.org/10.1016/j.envint.2017.01.018>
- 623 Lippiatt, S., Opfer, S., and Arthur, C., 2013. Marine debris monitoring and assessment. NOAA Technical Memo-  
624 randum NOS-OR&R-46.
- 625 Lithner, D., Larsson, Å., Dave, G., 2011. Environmental and health hazard ranking and assessment of plastic  
626 polymers based on chemical composition. *Sci. Total Environ.* 409, 3309–3324.  
627 <https://doi.org/10.1016/j.scitotenv.2011.04.038>
- 628 Löder, M.G.J., Gerdt, G., 2015. Methodology Used for the Detection and Identification of Microplastics—A  
629 Critical Appraisal, in: Bergmann, M., Gutow, L., Klages, M. (Eds.), *Marine Anthropogenic Litter*.  
630 Springer International Publishing, pp. 201–227.
- 631 Ludwig, W., Dumont, E., Meybeck, M., Heussner, S., 2009. River discharges of water and nutrients to the Medi-  
632 terranean and Black Sea: Major drivers for ecosystem changes during past and future decades? *Prog.*  
633 *Oceanogr.* 80, 199–217. <https://doi.org/10.1016/j.pcean.2009.02.001>
- 634 Ludwig, W., Probst, J.-L., 1996. A global modelling of the climatic, morphological, and lithological control of  
635 river sediment discharges to the oceans. *IAHS Publ.-Ser. Proc. Rep.-Intern Assoc Hydrol. Sci.* 236, 21–  
636 22.
- 637 Mani, T., Hauk, A., Walter, U., Burkhardt-Holm, P., 2015. Microplastics profile along the Rhine River. *Sci. Rep.*  
638 5. <https://doi.org/10.1038/srep17988>
- 639 Mani, T., Primpke, S., Lorenz, C., Gerdt, G., Burkhardt-Holm, P., 2019. Microplastic Pollution in Benthic Mid-  
640 stream Sediments of the Rhine River. *Environ. Sci. Technol.* 53, 6053–6062.  
641 <https://doi.org/10.1021/acs.est.9b01363>
- 642 Miller, R.Z., Watts, A.J.R., Winslow, B.O., Galloway, T.S., Barrows, A.P.W., 2017. Mountains to the sea: River  
643 study of plastic and non-plastic microfiber pollution in the northeast USA. *Marine Pollution Bulletin*  
644 124, 245–251. <https://doi.org/10.1016/j.marpolbul.2017.07.028>
- 645 MSFD Technical Subgroup on Marine Litter, 2013. Guidance on monitoring of marine litter in European seas.  
646 Joint Research Centre Scientific and Policy Reports, European Commission. 128 p.
- 647 Murphy, F., Ewins, C., Carbonnier, F., Quinn, B., 2016. Wastewater Treatment Works (WwTW) as a Source of  
648 Microplastics in the Aquatic Environment. *Environ. Sci. Technol.* 50, 5800–5808.  
649 <https://doi.org/10.1021/acs.est.5b05416>
- 650 Napper, I.E., Thompson, R.C., 2016. Release of synthetic microplastic plastic fibres from domestic washing  
651 machines: Effects of fabric type and washing conditions. *Mar. Pollut. Bull.* 112, 39–45.  
652 <https://doi.org/10.1016/j.marpolbul.2016.09.025>

- 653 Prevenios, M., Zeri, C., Tsangaris, C., Liubartseva, S., Fakiris, E., Papatheodorou, G., 2018. Beach litter dynam-  
654 ics on Mediterranean coasts: Distinguishing sources and pathways. *Mar. Pollut. Bull.* 129, 448–457.  
655 <https://doi.org/10.1016/j.marpolbul.2017.10.013>
- 656 Provencher, J.F., Ammendolia, J., Rochman, C.M., Mallory, M.L., 2018. Assessing plastic debris in aquatic food  
657 webs: what we know and don't know about uptake and trophic transfer. *Environ. Rev.*  
658 <https://doi.org/10.1139/er-2018-0079>
- 659 Rochman, C.M., Hoh, E., Kurobe, T., Teh, S.J., 2013. Ingested plastic transfers hazardous chemicals to fish and  
660 induces hepatic stress. *Sci. Rep.* 3, 3263. <https://doi.org/10.1038/srep03263>
- 661 Rochman, C.M., Tahir, A., Williams, S.L., Baxa, D.V., Lam, R., Miller, J.T., Teh, F.-C., Werorilangi, S., Teh,  
662 S.J., 2015. Anthropogenic debris in seafood: Plastic debris and fibers from textiles in fish and bivalves  
663 sold for human consumption. *Sci. Rep.* 5, 14340. <https://doi.org/10.1038/srep14340>
- 664 Rochman, C.M., 2018. Microplastics research—from sink to source. *Science* 360, 28–29.  
665 <https://doi.org/10.1126/science.aar7734>
- 666 Rodrigues, M.O., Abrantes, N., Gonçalves, F.J.M., Nogueira, H., Marques, J.C., Gonçalves, A.M.M., 2018. Spa-  
667 tial and temporal distribution of microplastics in water and sediments of a freshwater system (Antuã  
668 River, Portugal). *Sci. Total Environ.* 633, 1549–1559. <https://doi.org/10.1016/j.scitotenv.2018.03.233>
- 669 Sadaoui, M., Ludwig, W., Bourrin, F., Raimbault, P., 2016. Controls, budgets and variability of riverine sedi-  
670 ment fluxes to the Gulf of Lions (NW Mediterranean Sea). *J. Hydrol.* 540, 1002–1015.  
671 <https://doi.org/10.1016/j.jhydrol.2016.07.012>
- 672 Sadaoui, M., Ludwig, W., Bourrin, F., Romero, E., 2018. The impact of reservoir construction on riverine sedi-  
673 ment and carbon fluxes to the Mediterranean Sea. *Prog. Oceanogr.*, Special issue of MERMEX project:  
674 Recent advances in the oceanography of the Mediterranean Sea 163, 94–111.  
675 <https://doi.org/10.1016/j.pocean.2017.08.003>
- 676 Scheurer, M., Bigalke, M., 2018. Microplastics in Swiss Floodplain Soils. *Environ. Sci. Technol.* 52, 3591–98.  
677 <https://doi.org/10.1021/acs.est.7b06003>. Schmidt, C., Krauth, T., Wagner, S., 2017. Export of Plastic  
678 Debris by Rivers into the Sea. *Environ. Sci. Technol.* <https://doi.org/10.1021/acs.est.7b02368>
- 679 Schmidt, N., Thibault, D., Galgani, F., Paluselli, A., Sempéré, R., 2018. Occurrence of microplastics in surface  
680 waters of the Gulf of Lion (NW Mediterranean Sea). *Prog. Oceanogr.*, Special issue of MERMEX pro-  
681 ject: Recent advances in the oceanography of the Mediterranean Sea 163, 214–220.  
682 <https://doi.org/10.1016/j.pocean.2017.11.010>
- 683 Thompson, R.C., Olsen, Y., Mitchell, R.P., Davis, A., Rowland, S.J., John, A.W.G., McGonigle, D., Russell,  
684 A.E., 2004. Lost at Sea: Where Is All the Plastic? *Science* 304, 838–838.  
685 <https://doi.org/10.1126/science.1094559>
- 686 Tubau, X., Canals, M., Lastras, G., Rayo, X., Rivera, J., Amblas, D., 2015. Marine litter on the floor of deep  
687 submarine canyons of the Northwestern Mediterranean Sea: The role of hydrodynamic processes. *Prog.*  
688 *Oceanogr.* 134, 379–403. <https://doi.org/10.1016/j.pocean.2015.03.013>
- 689 Turner, A., Holmes, L.A., 2015. Adsorption of trace metals by microplastic pellets in fresh water. *Environ.*  
690 *Chem.* 12, 600–610. <https://doi.org/10.1071/EN14143>

- 691 Turner, S., Horton, A.A., Rose, N.L., Hall, C., 2019. A temporal sediment record of microplastics in an urban  
692 lake, London, UK. *J Paleolimnol* 61, 449–462. <https://doi.org/10.1007/s10933-019-00071-7>
- 693 UNEP 2003. Riverine transport of water, sediments and pollutants to the Mediterranean Sea. MAP  
694 Technical Reports Series No. 141, UNEP/MAP, Athens.
- 695 Zhou, Y., Liu, X., Wang, J., 2019. Characterization of microplastics and the association of heavy metals with  
696 microplastics in suburban soil of central China. *Science of The Total Environment* 694, 133798.  
697 <https://doi.org/10.1016/j.scitotenv.2019.133798>

Table 1. Main characteristics of the two sampled watersheds from the Gulf of Lion (NW Mediterranean Sea).

<b>Watershed characteristics</b>	<b>Rhône</b>	<b>Têt</b>
Watershed area (km <sup>2</sup> )	96364	1373
Length (km)	783	116
Population (10 <sup>6</sup> inhabitants)	9.3	0.3
Population density (inhabitants km <sup>-2</sup> )	97	165
Urban and other artificial land use (%)	4.8	5.1
Agricultural land use (%)	42.1	19.3
Forest (%)	36	36.6
Scrub and/ or herbaceous vegetation (%)	10.9	32.8
No vegetation (%)	6	6.1
Wetlands (%)	0.2	0.1
<b>Water and TSM discharge*</b>	<b>Rhône</b>	<b>Têt</b>
Long-term water discharge (m s <sup>-1</sup> )	1686	9.5
Long-term average TSM (mg L <sup>-1</sup> )	151	159
<b>Water and TSM discharge during sampling</b>	<b>Rhône</b>	<b>Têt</b>
Mean discharge (m <sup>3</sup> s <sup>-1</sup> )	1692	4.0
Min – max discharge (m <sup>3</sup> s <sup>-1</sup> )	356 – 8260	1 – 54
Mean TSM (mg L <sup>-1</sup> )	41	8
Min – max TSM (mg L <sup>-1</sup> )	2 – 4355	2 – 70

\* Sadaoui et al, 2016; TSM: Total Suspended Matter

Table 2. Means and ranges of MP concentrations in the Rhône and Têt rivers. \*The number of fiber is estimated from the weight of lint (see detail in section 2.3).

	<b>Rhône net</b>	<b>Rhône manta</b>	<b>Têt manta</b>	
Mean	19 ± 28	12 ± 18	42 ± 18	(Items m <sup>-3</sup> )
	0.5 ± 1.0	0.1 ± 0.2	0.8 ± 0.8	(mg m <sup>-3</sup> )
Min	2.4	0.3	0.8	(Items m <sup>-3</sup> )
	0.01	0.01	0.02	(mg m <sup>-3</sup> )
Max	88	59	618	(Items m <sup>-3</sup> )
	3.9	0.6	3.4	(mg m <sup>-3</sup> )
Total number of fibers*	3,584	44,448	143,654	(Items)
Total number of other shapes	259	853	11,151	(Items)

Table 3. Means and ranges of MP concentrations on the Têt shore and in atmospheric fallout.

	<b>Têt shore</b>		<b>Atmosphere fallout</b>	
Mean	258 ± 259	(Items kg <sup>-1</sup> )	22 ± 14	(Items m <sup>-2</sup> d <sup>-1</sup> )
	133 ± 125	(mg kg <sup>-1</sup> )		
Min	7.3	(Items kg <sup>-1</sup> )	5	(Items m <sup>-2</sup> d <sup>-1</sup> )
	3.95	(mg kg <sup>-1</sup> )		
Max	1,029	(Items kg <sup>-1</sup> )	65	(Items m <sup>-2</sup> d <sup>-1</sup> )
	458	(mg kg <sup>-1</sup> )		
Fiber	1,345	(Items)	926	(Items)
Other shapes	7,691	(Items)	0	(Items)

Table 4. Comparison of MP concentrations observed in river waters, on shores of European watersheds and in atmospheric fallout worldwide. Concentration values in brackets are maximum values.

Sites	Samples	Size range (mm)	Concentration	Reference
<b>Surface</b>			(Items m <sup>-3</sup> )	
Danube, Vienna (Austria)	1700	ND	0.31 ± 4.66 (147)	Lechner <i>et al.</i> (2014)
Rhine (Germany)	31	0.3-5	5 ± 4.96 (22)	Mani <i>et al.</i> (2015)
Seine, Paris (France)	3	0.3-5	0.35 (0.45)	Dris <i>et al.</i> (2015)
Rhône, Chancy (Switzerland)	5	0.3-5	0.29 ± 0.08	Faure <i>et al.</i> (2015)
Rhône, Arles (France)	8	0.8-5	0.19 (0.46)	Schimdt <i>et al.</i> (2018)
<i>Rhône, Arles (France)</i>	<i>15</i>	<i>0.3-5</i>	<i>19 ± 28 (88)</i>	<i>This study (net)</i>
<i>Rhône, Arles (France)</i>	<i>13</i>	<i>0.3-5</i>	<i>12 ± 18 (59)</i>	<i>This study (manta)</i>
<i>Têt, Villongue de la Sallanque (France)</i>	<i>35</i>	<i>0.3-5</i>	<i>42 ± 107 (618)</i>	<i>This study</i>
<b>Shore</b>			(Items kg <sup>-1</sup> )	
Rhine (Germany)	12	0.063-5	ND (3763)	Klein <i>et al.</i> (2015)
Main (Germany)	2	0.063-5	ND (1368)	Klein <i>et al.</i> (2015)
29 sites (Switzerland)	87	0.125-5	5 (593)	Scheurer and Bigalke (2018)
Kelvin (UK)	2	0.011-5	297 (432)	Blair <i>et al.</i> (2019)
<i>Têt, Canet-en-Roussillon (France)</i>	<i>33</i>	<i>0.063-5</i>	<i>258 ± 259 (1,029)</i>	<i>This study</i>
<b>Atmospheric fallout</b>			(Items m <sup>-2</sup> d <sup>-1</sup> )	
Paris (France)	24	>0.1	110 ± 96 (355)	Dris <i>et al.</i> (2016)
Paris (France)	24	>0.1	53 ± 38 (114)	Dris <i>et al.</i> (2016)
Donggun city (China)	9	>0.1	228 ± 43 (313)	Cai <i>et al.</i> (2017)
Bernadouze (France)	10	0.001-5	365 ± 69 (462)	Allen <i>et al.</i> (2019)
Hambourg (Germany)	108	0.001-5	275*	Klein and Fischer (2019)
<i>Perpignan (France)</i>	<i>28</i>	<i>0.063-5</i>	<i>22 ± 14 (65)</i>	<i>This study</i>

\* median value

**Figure**

[Click here to download Figure: Figures-constant\\_2019.doc](#)

Figure 1: Location maps of the study areas. A) General map of the Mediterranean Sea with the NW Mediterranean part in shaded area. B) Both sampling areas (shaded areas) of the Têt and the Rhône river basins. C) The sampling site on the Rhône River. D) The sampling site on the Têt River. Grey numbered diamonds represent locations of both weather stations of Perpignan (1) and Arles (4), both gauging stations of Villelongue-de-la-Salanque (2; Têt) and Beaucaire (3; Rhône) and the TSM sampling sites of Villelongue-de-la-Salanque and Arles. The green pentagon indicates the atmospheric sampling site (Perpignan), blue-green circles designate both river sampling sites (Villelongue-de-la-Salanque and Arles) and the pink triangle points out the river shore sampling site at the Têt mouth.

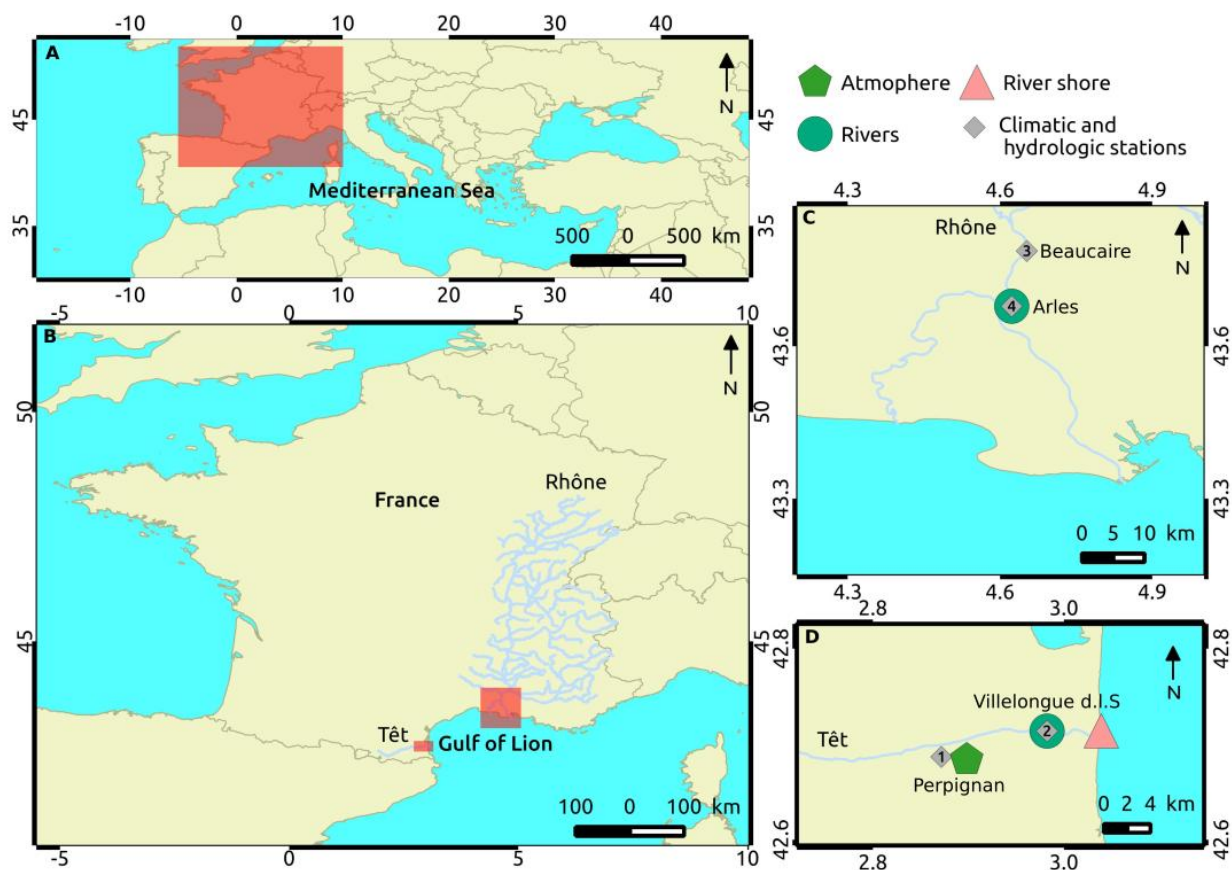


Figure 2. MP concentrations in the Rhône and the Têt river basins expressed in items  $m^{-3}$  (A-C), items  $kg^{-1}$  (D),  $mg m^{-3}$  (E-G) and  $mg kg^{-1}$  (H). A, E) Mean concentrations in the Rhône and Têt rivers surface water (see period details in section 2.2). B,F) Mean concentrations at two river positions (center and right) of the Rhône River surface water and using two conical nets (see period details in section 2.2). C,G) Concentrations in the Têt River surface water during 9 monthly sampling periods (from December 2015 to October 2016) where triplicates were performed with the Manta trawl. D, H) Mean concentrations at four shoreline sediment stations (quadra) along the Têt River's mouth, repeated 8 times from October 2015 to February 2017. Statistical significance of differences: ns = non significant difference ( $p$ -value  $>0.05$ ), \* = significant ( $p$ -value  $<0.05$ ), \*\* = highly significant ( $p$ -value  $<0.01$ ), \*\*\* = very highly significant ( $p$ -value  $<0.001$ ).

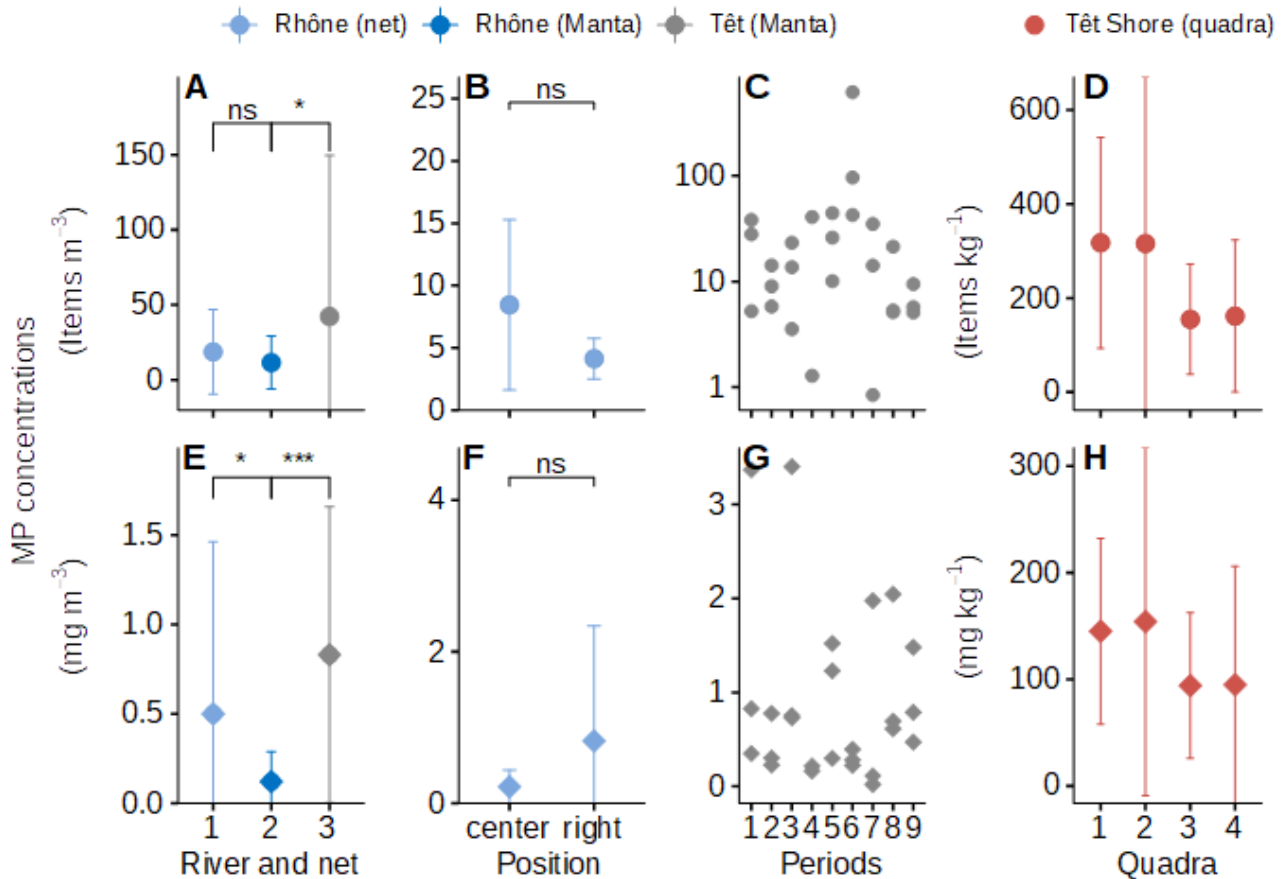


Figure 3. Relative shape distribution and synthetic organic polymer composition of MPs found in both rivers (Rhône and Têt), in the shore sediments of the Têt mouth and in atmospheric deposits at Perpignan. Shapes: fibers, fragments, foams, films and beads. Polymers: polyethylene (PE), polypropylene (PP), polystyrene (PS), polyester (PES), polyamide (PA), acrylic (A), other plastics (polyvinyl chloride, polyethylene-vinyl acetate, polyethylene terephthalate, polyurethane), unidentified and non plastics determined after FTIR spectrometer analysis (see details in section 2.3). Notice differences in % scale between matrices for fragments, foams, films and beads.

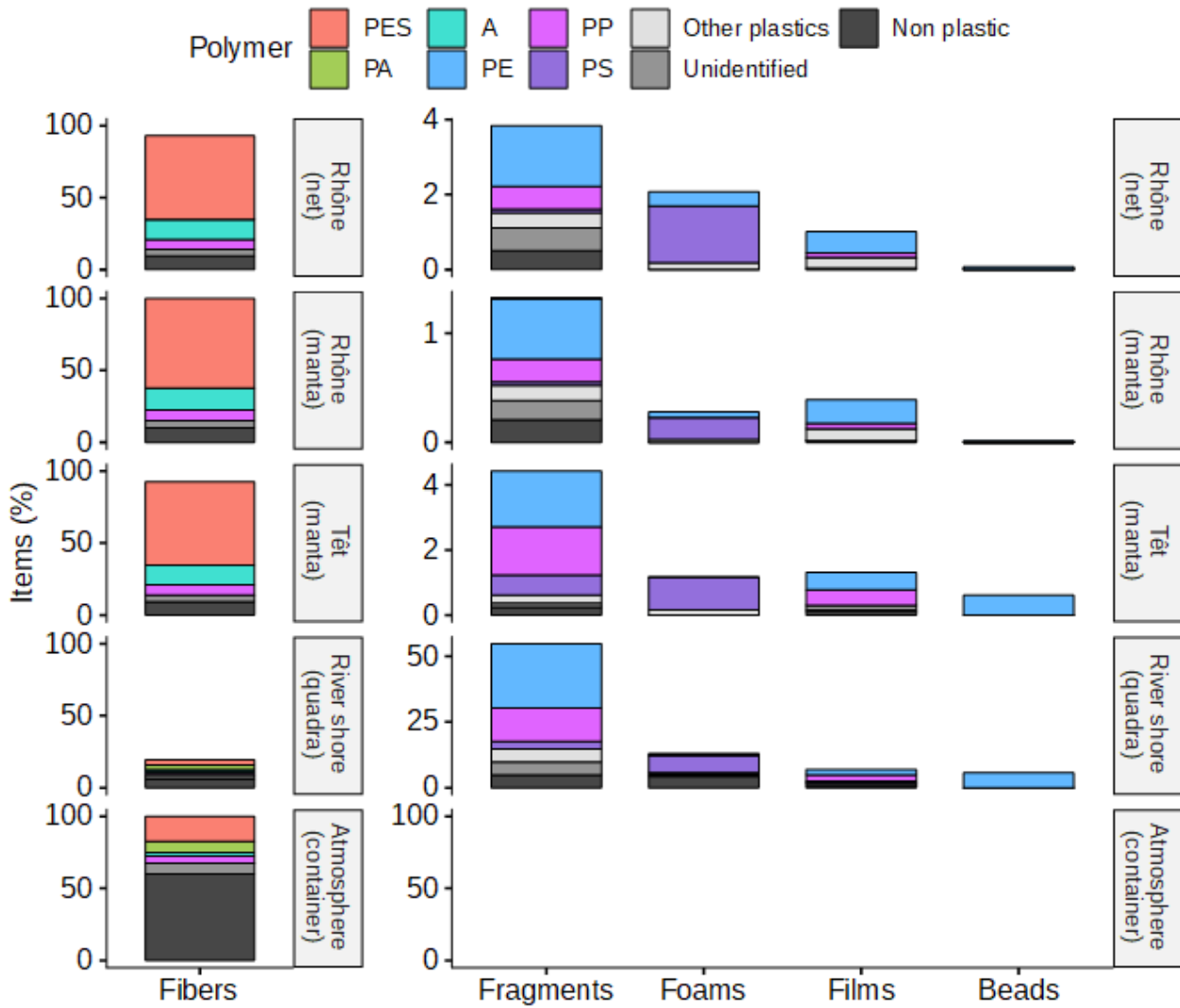


Figure 4. Temporal evolution (from Oct. 2015 to July 2017) of MP concentrations from the Rhône River (Arles station) in relation with hydrological and meteorological parameters. A) Numerical concentration of MPs (items  $m^{-3}$ ). B) Mass concentration of MPs ( $mg m^{-3}$ ). C) Rhône River flow rate ( $m^3 s^{-1}$ ; measured at Beaucaire: 43.8045752 N, 4.6491328 E; data from Hydro service) and Total Suspended Matter or TSM ( $mg L^{-1}$ ; measured at Arles: 43.679019 N, 4.623012 E). D) Precipitation (in mm) measured at Arles (43.5100000 N, 4.6933333 E), data from Publithèque (2018). Blue points represent Manta trawl samples and yellow points conical net samples.

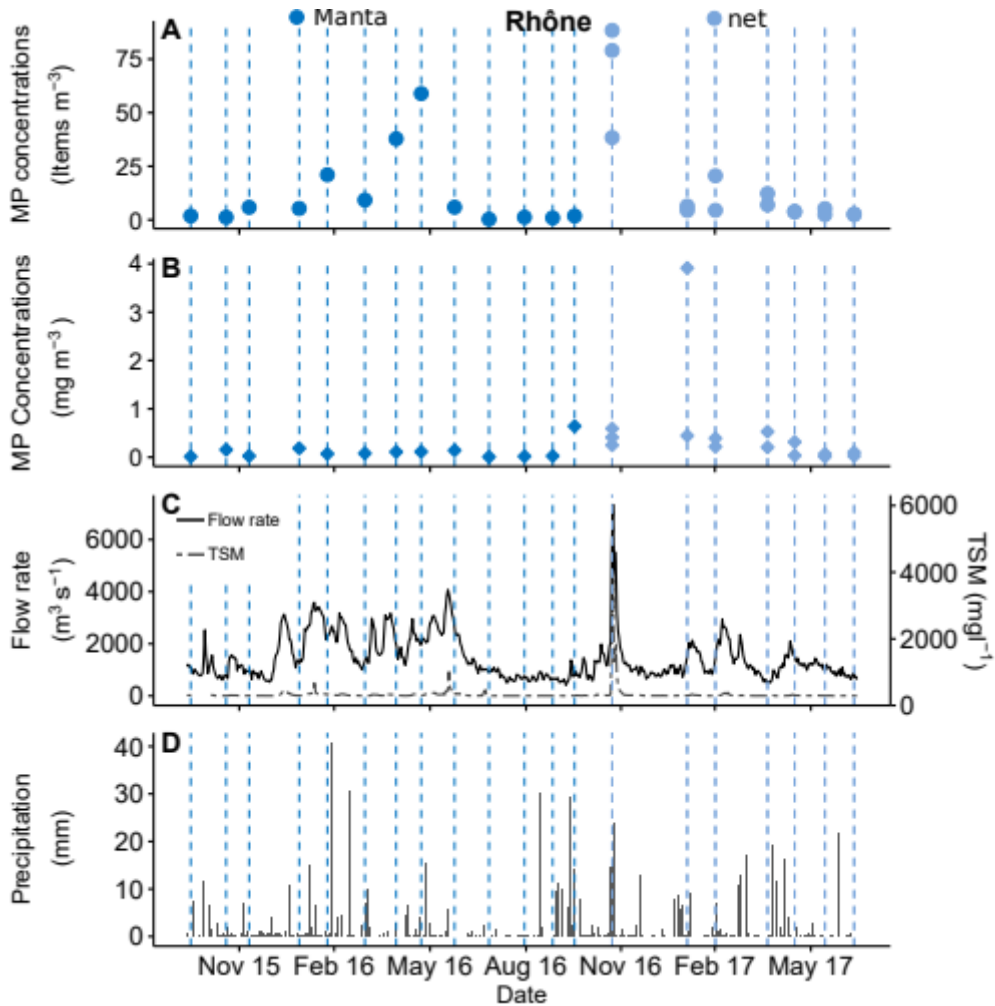


Figure 5. Temporal evolution (from Oct. 2015 to Feb. 2017) of MP concentrations from the Têt River in relation with hydrological and meteorological parameters. A and B) numerical (items  $m^{-3}$ ) and mass ( $mg\ m^{-3}$ ) concentrations of MPs in the Têt waters (Villalongue-de-la-Salanque station), respectively. C and D) numerical (items  $m^{-3}$ ) and mass ( $mg\ m^{-3}$ ) concentrations of MPs along the shore at the Têt mouth, respectively. E) Têt River flow rate ( $m^3\ s^{-1}$ ; measured at Perpignan: 42.7034175 N, 2.8930531 E; data from Hydro service) and Total Suspended Matter or TSM ( $mg\ L^{-1}$ ; measured at Villalongue-de-la-Sallanque: 42.713738 N, 2.982379 E). F) Precipitation in mm, measured at Perpignan (42.7366667 N, 2.8716667 E), data from Publithèque (2018).

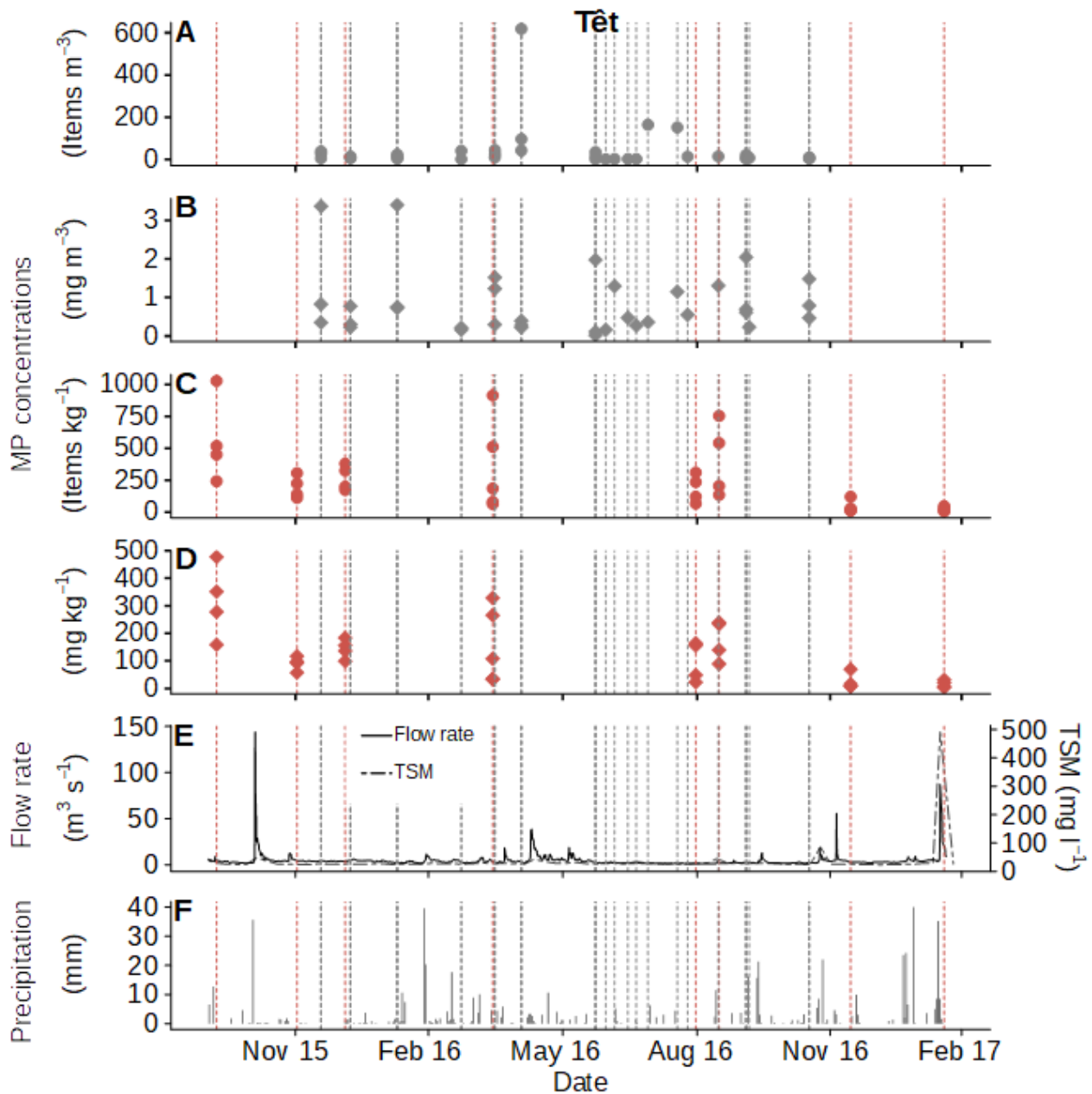


Figure 6. Relationships between MP concentrations and external parameters. A-F) Samples from the Rhône River expressed in items  $m^{-3}$  (A-C) and  $mg m^{-3}$  (D-F). G-L) Samples from the Têt River expressed in items  $m^{-3}$  (G-I) and  $mg m^{-3}$  (J-L). Concentration are plotted against the flow rate (A, D, J, G;  $m^3 s^{-1}$ ), precipitation (B, E, H, K; mm) and TSM (C, F, I, L;  $mg L^{-1}$ ) occurring during the same sampling day. M, N) Atmospheric fallout samples from Perpignan (items  $m^{-2} d^{-1}$ ) according to cumulated daily precipitation (M; mm) and daily mean wind (N;  $m s^{-1}$ ).

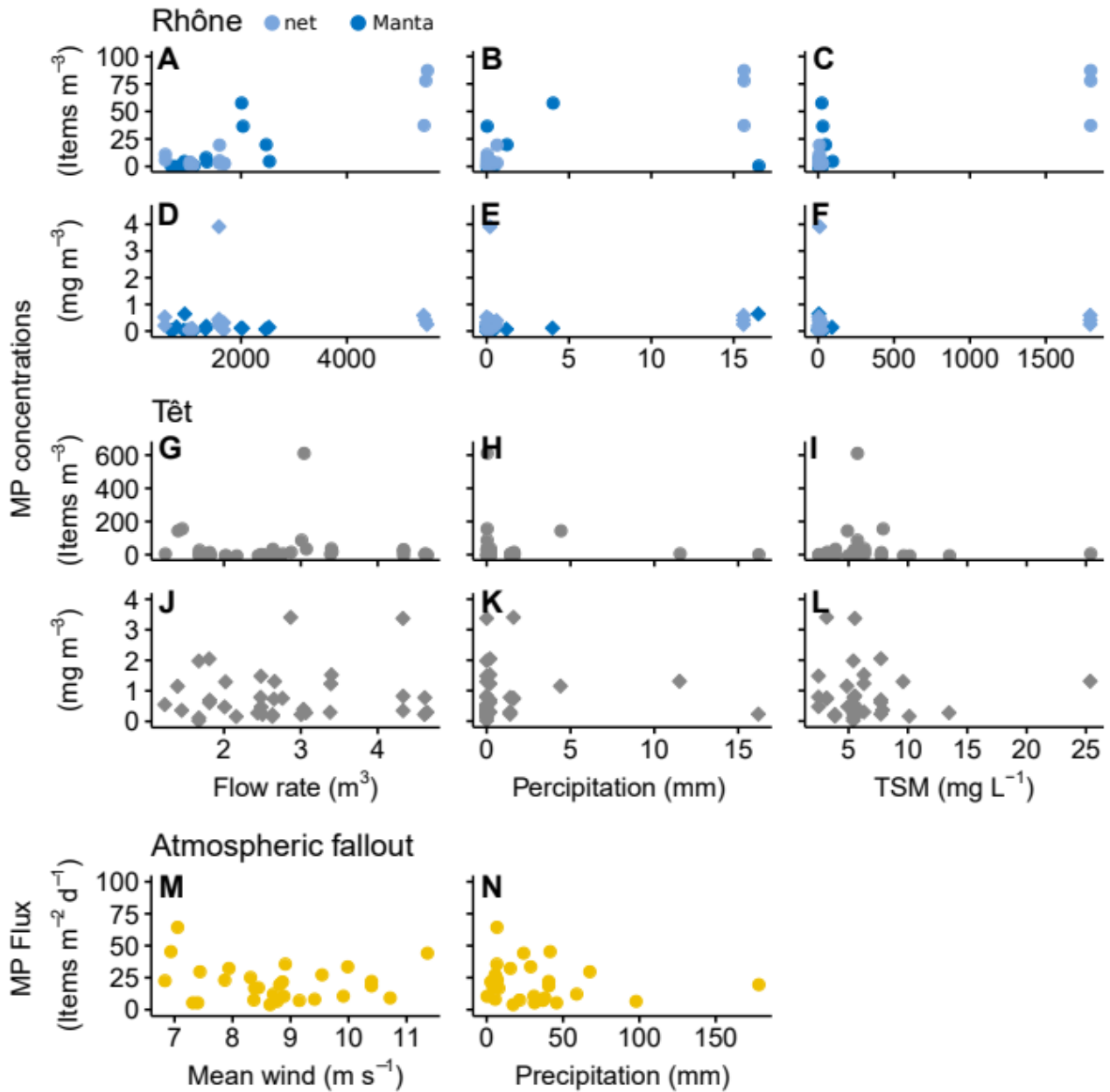


Figure 7. Temporal evolution (from Oct. 2015 to Feb. 2018) of MP flux and precipitation. A) MP flux within atmospheric fallout (items  $m^{-2} d^{-1}$ ) at Perpignan in relation. B) Daily (barplot) and cumulated precipitation (in mm) for each sampling intervals (line). Precipitation at Perpignan, data from Publithèque (2018).

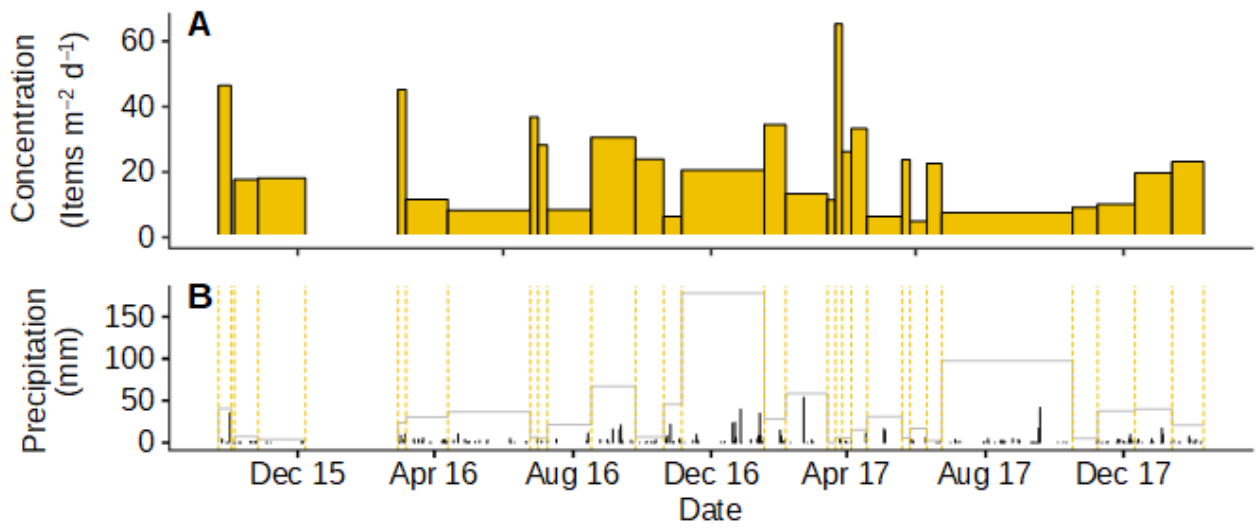


Figure 8. Relationship between the Log *ratio* mass MPs on mass TSM from the Rhône and the Têt Rivers according to Log of TSM ( $\text{mg L}^{-1}$ ).

